Stress concentrations around shallow spherical depressions in a flat plate

Cowper, G. R.

Publisher's version / Version de l'éditeur:
https://doi.org/10.4224/40003675
Aeronautical Report (National Research Council Canada. National Aeronautical Establishment. Structures Laboratory); no. LR-340, 1962-04

NATIONAL RESEARCH COUNCIL OF CANADA

AERONAUTICAL REPORT

LR - 340

STRESS CONCENTRATIONS AROUND SHALLOW SPHERICAL DEPRESSIONS IN A FLAT PLATE

BY

G. R. COWPER

NATIONAL AERONAUTICAL ESTABLISHMENT

OTTAWA

APRIL 1962

N. R. C. NO. 6857

NATIONAL RESEARCH LABORATORIES

Ottawa, Canada

REPORT

National Aeronautical Establishment

Structures Laboratory

Pages - Preface - 4
Text - 34
Tables - 13
Figures - 14

Report: LR-340
Date: April 1962
Lab. Order: NAE-730
File: M49-7-40

For: Internal

Subject: STRESS CONCENTRATIONS AROUND SHALLOW SPHERICAL DEPRESSIONS IN A FLAT PLATE

Submitted by: A.H. Hall
Section Head

Author: G.R. Cowper

Approved by: F.R. Thurston
Director

SUMMARY

A theoretical elastic stress analysis is given of an infinite flat plate which is loaded in uniaxial tension and which is weakened by two shallow spherical depressions cut symmetrically into each surface of the plate. Results are presented in the form of (i) tabulated functions from which the stresses and stress gradients at any significant point can be calculated, and (ii) graphs which illustrate the main features of the stress distribution.

TABLE OF CONTENTS

LIST OF TABLES

LIST OF TABLES (Cont'd)

LIST OF ILLUSTRATIONS

LIST OF ILLUSTRATIONS (Cont'd)

STRESS CONCENTRATIONS AROUND SHALLOW SPHERICAL DEPRESSIONS IN A FLAT PLATE

1.0 INTRODUCTION

A specimen of the type shown in Figure 1 has been suggested as possibly being useful in certain crack-propagation studies. As can be seen from the figure the specimen is a flat plate which is loaded in tension and in which a region of stress concentration is produced by cutting two shallow spherical depressions symmetrically into each face of the plate. A feature of such a specimen is that the point of maximum stress is entirely surrounded by a region of lower stress. Since a crack initiated at the point of maximum stress can therefore propagate only into a region of lower stress it may be expected that the growth of the crack is a stable process and that the growth can be controlled by altering the tension on the specimen. Moreover, the stress gradients in the central region of the specimen can be altered, to a certain extent, by varying the depth of the depressions. These are the reasons for interest in this type of specimen.

The present report supplies data on the stress concentrations and stress gradients which exist in a virgin specimen, the information being obtained from a mathematical stress analysis based on the theory of elasticity. To make the problem tractable two main simplifying assumptions are introduced. These are, first, that the width of the specimen is sufficiently large compared with the diameter of the depression that the specimen may be treated as an infinite plate, and second, that the plate is sufficiently thin that it is in a state of plane stress. In addition, a minor approximation relating to the form of the depression is introduced. In the

body of the report the method of analysis is outlined and graphs of stresses and stress gradients are presented and discussed.

2.0 MATHEMATICAL FORMULATION OF PROBLEM

The coordinate system used is shown in Figure 1. Standard notations are used for stresses, displacements, and elastic moduli.

In keeping with the assumption that the specimen is in a state of plane stress, it is assumed that the stresses are uniform across the thickness of the plate. The equations for equilibrium of an element of the plate in the radial and circumferential directions then are (Ref. 2)

$$r\frac{\partial \sigma_{rr}}{\partial r} + \frac{\partial \sigma_{r\theta}}{\partial \theta} + \left(1 + \frac{r}{t}\frac{dt}{dr}\right)\sigma_{rr} - \sigma_{\theta\theta} = 0$$

$$r\frac{\partial \sigma_{r\theta}}{\partial r} + \frac{\partial \sigma_{\theta\theta}}{\partial \theta} + \left(2 + \frac{r}{t}\frac{dt}{dr}\right)\sigma_{r\theta} = 0 \qquad (1)$$

For plane stress in polar coordinates, Hooke's law is expressed by (Ref. 4)

$$E\frac{\partial u_r}{\partial r} = \sigma_{rr} - \nu\sigma_{\theta\theta}$$

$$E\left(\frac{1}{r}\frac{\partial u_\theta}{\partial \theta} + \frac{u_r}{r}\right) = \sigma_{\theta\theta} - \nu\sigma_{rr} \qquad (2)$$

$$E\left(\frac{1}{r}\frac{\partial u_r}{\partial \theta} - \frac{u_\theta}{r} + \frac{\partial u_\theta}{\partial r}\right) = 2(1+\nu)\,\sigma_{r\theta}$$

The assumptions that the displacements are uniform across the thickness of the plate and that the stress normal to the plane of the plate is negligible are implicit in (2).

The thickness of the plate in the region $r \leq a$ (Fig. 1) is determined by the specified spherical shape of the depressions. However, since the exact expression for the thickness is cumbersome, it is worth while to substitute an approximate but simpler expression for the exact relation. We therefore assume that the thickness of the plate is given by

$$t = \begin{cases} t_1 \left[1 + \left(\frac{t_o - t_1}{t_1}\right)\left(\frac{r}{a}\right)^2\right], & r \leq a \\ t_o, & r \geq a \end{cases} \tag{3}$$

The expression (3) is a good approximation to the exact spherical shape provided the diameter of the depressions is greater than four or five times the thickness of the plate.

As stated in the introduction it is assumed that the specimen is sufficiently wide that it can be treated as an infinite plate. Then the stress boundary conditions are that at large distances from the depressions the stress field should tend to a uniaxial tension of magnitude σ_o in the direction $\theta = 0$. Expressing this condition in polar coordinates yields

$$\begin{aligned} \sigma_{rr} &\to (\sigma_o/2)(1 + \cos 2\theta) \\ \sigma_{\theta\theta} &\to (\sigma_o/2)(1 - \cos 2\theta) \\ \sigma_{r\theta} &\to -(\sigma_o/2) \sin 2\theta \end{aligned} \tag{4}$$

as $r \to \infty$. In addition the stress components σ_{rr} and $\sigma_{r\theta}$ and the displacements u_r and u_θ must be continuous at the edge of the depression $r = a$.

Equations (1), (2), and (3) with the boundary conditions (4) constitute the mathematical formulation of our stress analysis problem. We pass over, for the moment, the somewhat involved procedures needed to solve the equations and turn to a consideration of the results. Suffice it to say here that the mathematical and computational work introduces no further approximations.

3.0 RESULTS AND DISCUSSION

The solution of the foregoing equations yields the formulas

$$\begin{aligned} \sigma_{rr}/\sigma_o &= f_o(\rho) + f_2(\rho) \cos 2\theta \\ \sigma_{\theta\theta}/\sigma_o &= g_o(\rho) + g_2(\rho) \cos 2\theta \\ \sigma_{r\theta}/\sigma_o &= h_2(\rho) \sin 2\theta \end{aligned} \qquad (5)$$

where f_o, f_2, g_o, g_2, h_2 are functions of the non-dimensional radial coordinate $\rho \equiv r/a$, of the ratio $q \equiv t_1/t_o$ which is a measure of the depth of the depressions, and of Poisson's ratio. These functions and their derivatives with respect to ρ are tabulated in Tables IV to XIII for the ranges $\rho = 0(0.1)2.0$, $q = 0(0.2)1.0$, and the single value of Poisson's ratio $\nu = 0.3$. By use of the tables and formulas (5) all stresses and stress gradients at any significant point in the plate can be found.

An over-all picture of the stress distribution is given in Figures 2 and 3 in which stresses are plotted for the case $q = 0.2$. Because of symmetry the stresses in only one gradrant of the plate need be plotted. Although the stress formulas are simplest when polar components of stress are used, as in (5), the stress distribution is most easily understood when stresses are expressed in rectangular Cartesian components. Accordingly it is the Cartesian stress components σ_{xx}, σ_{yy}, σ_{xy} which are plotted in Figures 2 and 3. We note that the stress σ_{xx} predominates. The graph of σ_{xx} (Fig. 2) has a smooth hump centred over the depressions, while in the region outside the depressions σ_{xx} tends gradually to its asymptotic value σ_o. The stresses σ_{xy} and σ_{yy} are comparatively small. In the case illustrated ($q = 0.2$), σ_{xy} is always less than 12 percent of σ_o, while σ_{yy} is always less than 14 percent of σ_o.

The effect of varying the depth of the depressions is shown in Figures 4, 5, and 6, in which the stresses along the x- and y-axes are plotted for a range of values of q. (Recall $q \equiv t_1/t_o$.) As could be expected the peak stress increases as q decreases, and moreover the peak stress becomes infinite as q tends to zero. Figure 6 again shows that the stress σ_{yy} is comparatively small. In Figure 5 it is interesting to note that the stress σ_{rr} on the x-axis falls to a value less than σ_o at $\rho \doteq 1$. As ρ increases beyond 1 this stress gradually rises to σ_o.

An indication of the nature of the stress gradients is given by Figures 7 and 8. Here the radial gradients of the predominant stress σ_{xx} along the x- and y-axes are plotted. Note that the stress gradients are discontinuous at the edge of the depressions; indeed the gradient $\partial\sigma_{rr}/\partial r$ along the x-axis even changes sign there (Fig. 8). A curious feature

of Figure 8 is that the curve for q = 0 appears to pass through the peaks of the curves for other values of q. As far as the author is aware, this is pure coincidence.

By superposition of the results (5) for uniaxial tension at infinity the stress field due to equal biaxial tensions at infinity can be obtained. In this case the stress field is axisymmetric and the stresses are given by

$$\sigma_{rr}/\sigma_o = 2f_o(\rho)$$
$$\sigma_{\theta\theta}/\sigma_o = 2g_o(\rho) \qquad (6)$$
$$\sigma_{r\theta} = 0$$

These quantities are plotted in Figures 9 and 10, and their radial gradients are plotted in Figures 11 and 12. The curves are quite similar to the curves of Figures 4, 5, 7, and 8, respectively. Despite this similarity the stress distributions are quite different in the two cases of uniaxial tension and biaxial tension at infinity, as a comparison of (5) and (6) shows. Stresses due to other combinations of loads at infinity can of course be obtained by suitable superpositions.

Finally, we emphasize that the results in this report apply only to an uncracked specimen.

4.0 EFFECT OF SIMPLIFYING ASSUMPTIONS

To make the problem tractable three simplifying assumptions were introduced: (i) the plate is infinitely large, (ii) the plate is in a state of plane stress, (iii) the thickness in the region of the depressions is given by

$$t = t_1 + (t_o - t_1)(r/a)^2 \qquad (7)$$

We will now try to estimate the errors which these assumptions introduce

4.1 Effect of Finite Width

Consider a plate of finite width w containing depressions (Fig. 13a). Let us write the stresses in the plate in the form

$$\begin{aligned} \sigma_{xx} &= \sigma^1_{xx} + \sigma^2_{xx} \\ \sigma_{yy} &= \sigma^1_{yy} + \sigma^2_{yy} \\ \sigma_{xy} &= \sigma^1_{xy} + \sigma^2_{xy} \end{aligned} \qquad (8)$$

where σ^1_{xx}, σ^1_{yy}, σ^1_{xy} are the stresses given by the infinite plate solution while σ^2_{xx}, σ^2_{yy}, σ^2_{xy} are the corrections for the effect of finite width. The stresses σ^2_{xx}, σ^2_{yy}, σ^2_{xy} must satisfy the usual conditions of equilibrium and compatibility and must be such as to make the edges of the plate free of traction. Hence on the edges ABC, DEF, (Fig. 13) we have

$$\sigma^2_{yy} = -\sigma^1_{yy}, \qquad \sigma^2_{xy} = -\sigma^1_{xy} \qquad (9)$$

Moreover σ^2_{xx}, σ^2_{yy}, σ^2_{xy} decrease to zero in remote regions of the plate. The task of finding σ^2_{xx}, σ^2_{yy}, σ^2_{xy} therefore amounts to solving for the stresses in a plate loaded as shown in Figure 13b.

An exact solution for σ^2_{xx}, σ^2_{yy}, σ^2_{xy} would be extremely difficult, and the best we can do is make some rather crude

estimates of their magnitude. The magnitude of σ^2_{xx}, σ^2_{yy}, σ^2_{xy} is of course directly related to the magnitude of the boundary values of σ^2_{yy}, σ^2_{xy} on the edges ABC, DEF, and the latter decrease as q increases and as the ratio w/2a increases. In the calculations which follow we take q = 0.2 assuming that this is probably the lowest value of q reasonably obtainable in practice.

In estimating σ^2_{xx}, σ^2_{yy}, σ^2_{xy} it is convenient to split the loading of Figure 13b into two parts, namely, (i) the normal tractions and (ii) the shear tractions, and to consider separately the effect of each part. Consider first the plate loaded only by normal tractions - σ^1_{yy} on the edges ABC, DEF. It seems reasonable to assume that this loading causes chiefly a stress σ^2_{yy} while the stresses σ^2_{xx}, σ^2_{xy} are comparatively small.* The largest correction σ^2_{yy}, no doubt occurs at the centre of the depressions. If there were no depressions in the plate we might assume that the boundary tractions are transmitted through the plate without substantial change, so that the stress σ^2_{yy} at O is the same as at the points B and E. To allow for the stress concentrating effect of the depressions we introduce a factor of 2.5, which is the stress concentration factor for the infinite plate when q = 0.2. Thus the estimated largest value of σ^2_{yy} is 2.5 times the value of σ^1_{yy} at the points B or E.

Now consider the plate of Figure 13b loaded only by shear tractions. Under this loading a resultant force is transmitted across transverse sections of the plate and across section BE in particular. It seems reasonable to

---

* Compare the discussion of stresses in a long beam under a similar loading in Reference 5.

suppose that this loading results chiefly in stresses σ^2_{xx} and σ^2_{xy} while σ^2_{yy} is comparatively small. The largest correction σ^2_{xx} probably occurs at the centre of the depression. To estimate its magnitude we calculate the force P transmitted across section BE. The average stress on BE then is P/wt_o, ignoring the presence of the depressions. To allow for the stress concentrating effect of the depressions we again apply a factor of 2.5 and thus arrive at $2.5\ P/wt_o$ as an estimate of the largest value of the correction σ^2_{xx}. As for σ^2_{xy}, we assume it is never larger than the maximum value of σ^2_{xy} on the edges ABC, DEF.

Numerical values of the estimated largest corrections for the effect of finite width are presented in Table I below. As stated before the figures apply to the case $q = 0.2$. For larger values of q smaller corrections can be expected. The last line of the table gives the estimated correction to σ_{xx} as a percentage of the largest value of σ_{xx}.

TABLE I

ESTIMATED CORRECTIONS FOR FINITE WIDTH

w/2a	2	3	5	10
Correction to σ_{xx}/σ_c	0.090	0.035	0.013	0.003
Correction to σ_{yy}/σ_c	0.150	0.078	0.033	0.008
Correction to σ_{xy}/σ_o	0.021	0.012	0.005	0.001
Relative error in σ_{xx}, %	3.6	1.4	0.5	0.1

We conclude that the error in σ_{xx} as given by the infinite plate solution is probably not more than 3 or 4 percent if the width of the plate is twice the diameter of the depressions, and is probably not more than 1 or 2 percent if the width is three times the diameter. Somewhat larger errors may occur in the relatively small stresses σ_{xy} and σ_{yy}.

4.2 Assumption of Plane Stress

The assumption of plane stress conditions involves, in fact, two assumptions; first, that the major stresses and displacements are uniform across the thickness of the plate, and second, that the stress normal to the plane of the plate is negligible. In order to see what errors these assumptions can cause, we examine two particular plates for which exact solutions are available, and hence for which the errors of an approximate plane stress solution can be deduced. The plates examined are a wedge-shaped semi-infinite plate and an infinite plate whose surfaces are two shallow hyperbolic cylinders, both plates being loaded in uniaxial tension. Figure 14 shows portions of these plates together with a comparison section of a plate with depressions. The plate of Figure 14(a) will be referred to as plate A and the plate of Figure 14(b) as plate B. In order for conditions in these plates to be comparable with conditions in a plate with spherical depressions we make the semi-angle α of plate A equal to the maximum slope of the surface of the depression, and we make the minimum radius of curvature ρ of the surface of plate B equal to the spherical radius of the depressions. (See Fig. 14). This fixes the values of α and ρ as

$$\alpha = (1 - q)(t_o/a), \qquad \rho = R = a^2/(1 - q)t_o \qquad (10)$$

Then it is not unreasonable to suppose that conditions in plate A are somewhat representative of conditions near the edge of the depressions, while conditions in plate B are somewhat representative of conditions near the centre of the depressions.

The exact solutions for plates A and B are given in References 3 and 6, while the approximate plane stress solutions are easily found since they are, in effect, statically determinate. The essential results of a comparison of the exact and approximate solutions are as follows. The plane stress theory correctly predicts the average stress across the thickness of the plate even though the stresses are not uniform across the thickness. The greatest discrepancy between exact and approximate solutions occurs at the faces of the plate. For plate A the stress σ_{xx} at the faces of the plate is less than that predicted by plane stress theory, the relative error being approximately

$$(4/3)(1 - q)^2(t_o/a)^2 \qquad (11)$$

when a is given by (10). The opposite situation occurs in plate B, for at the section of minimum thickness the stress σ_{xx} at the faces of the plate is larger than that predicted by plane stress theory. Here the relative error is approximately

$$(1/3)q(1 - q)(t_o/a)^2 \qquad (12)$$

The size of these errors is tabulated in Tables II and III

below.

TABLE II

RELATIVE ERROR IN PLANE STRESS SOLUTION FOR PLATE A

a/t_o	2	3	5	10
Error, %; q = 0.5	8.3	3.7	1.3	0.3
Error, %; q = 0.2	21	9.5	3.4	0.9

TABLE III

RELATIVE ERROR IN PLANE STRESS SOLUTION FOR PLATE B

a/t_o	2	3	5	10
Error, %; q = 0.5	2.1	0.9	0.3	0.1
Error, %; q = 0.2	1.3	0.6	0.2	0.1

It should also be mentioned that a more rigorous theory which is free of the assumptions of plane stress is available for plates of constant thickness (Ref. 7). This theory can be applied to the region of the plate outside the depressions and corrections to the plane stress solution in that region can be obtained. Once again the correction is proportional to $(t_o/a)^2$. When q is larger than 0.2 the correction is not more than 1.2 percent of σ_o if $a \geq 2t_o$, and

is not more than 0.5 percent of σ_o if $a \geq 3t_o$.

In summary, it appears that the error introduced by the assumption of plane stress is proportional to $(t_o/a)^2$. On the basis of the results for plate B we estimate that the error in the stress at the centre of the plate is probably not more than 2 or 3 percent if $a \geq 2t_o$, and is probably not more than 1 or 2 percent if $a \geq 3t_o$. The results for plate A indicate that larger errors may occur in the less critical region of the edge of the depression.

4.3 Approximate Expression for Thickness

For an exactly spherical depression of outer radius a and such that the thickness of the plate at the centre is t_1, the correct expression for the thickness is

$$t = t_1 + 2R - 2\sqrt{R^2 - r^2} \qquad (13)$$

where the spherical radius R is given by

$$R = a^2/(t_o - t_1) + (t_o - t_1)/4 \qquad (14)$$

The maximum difference d between (13) and the approximate expression (7) is

$$d = t_o(1 - q)^3(t_o/4a)^2 \qquad (15)$$

Hence, when $q = 1/2$, d is less than 1 percent of t_o if $a > t_o$, and when $q = 0$, d is less than 1 percent of t_o if $a > 5t_o/2$. It appears that (7) is an adequate approximation to the shape of the depressions provided the diameter of the depressions is greater than, say, four or five times the thickness of the plate.

5.0 MATHEMATICAL DETAILS

5.1 Solution of Governing Equations

The governing equations obtained in section 2 are

$$r\frac{\partial \sigma_{rr}}{\partial r} + \frac{\partial \sigma_{r\theta}}{\partial \theta} + \left(1 + \frac{r}{t}\frac{dt}{dr}\right)\sigma_{rr} - \sigma_{\theta\theta} = 0$$

$$r\frac{\partial \sigma_{r\theta}}{\partial r} + \frac{\partial \sigma_{\theta\theta}}{\partial \theta} + \left(2 + \frac{r}{t}\frac{dt}{dr}\right)\sigma_{r\theta} = 0$$

$$E\frac{\partial u_r}{\partial r} = \sigma_{rr} - \nu\sigma_{\theta\theta} \qquad (16)$$

$$E\left(\frac{1}{r}\frac{\partial u_r}{\partial \theta} - \frac{u_\theta}{r} + \frac{\partial u_\theta}{\partial r}\right) = 2(1+\nu)\sigma_{r\theta}$$

$$E\left(\frac{1}{r}\frac{\partial u_\theta}{\partial \theta} + \frac{u_r}{r}\right) = \sigma_{\theta\theta} - \nu\sigma_{rr}$$

where t is given by

$$t = \begin{cases} t_1\left[1 + \left(\dfrac{t_o - t_1}{t_1}\right)\left(\dfrac{r}{a}\right)^2\right], & r \le a \\ t_o, & r \ge a \end{cases} \qquad (17)$$

The boundary conditions are

$$\begin{aligned} \sigma_{rr} &\to (\sigma_o/2)(1 + \cos 2\theta) \\ \sigma_{\theta\theta} &\to (\sigma_o/2)(1 - \cos 2\theta) \\ \sigma_{r\theta} &\to -(\sigma_o/2) \sin 2\theta \end{aligned} \tag{18}$$

as $r \to \infty$. Further, the stresses σ_{rr} and $\sigma_{r\theta}$ and the displacements u_r and u_θ must be continuous at $r = a$.

We can find solutions of (16) by supposing that all unknown quantities are of the form $f(r) \cos m\theta$ or $f(r) \sin m\theta$ where m is an integer. Accordingly let

$$\begin{aligned} \sigma_{rr} &= \sigma_o S_{rr}(r) \cos m\theta \\ \sigma_{\theta\theta} &= \sigma_o S_{\theta\theta}(r) \cos m\theta \\ \sigma_{r\theta} &= \sigma_o S_{r\theta}(r) \sin m\theta \\ u_r &= (\sigma_o r/E) w_r(r) \cos m\theta \\ u_\theta &= (\sigma_o r/E) w_\theta(r) \sin m\theta \end{aligned} \tag{19}$$

where appropriate factors have been introduced to make the quantities S_{rr}, w_r, etc., non-dimensional. Note that u_r and u_θ have been non-dimensionalized in terms of the variable radius r instead of the fixed radius a. This simplifies subsequent equations. Define the non-dimensional radius ρ by $\rho = r/a$, and put $q = t_1/t_o$. By substituting (17) and (19) into (16) the non-dimensional governing equations for S_{rr}, w_r,

etc., are found to be

$$\begin{aligned}
\rho dS_{rr}/d\rho &= -(1 + F(\rho))\, S_{rr} + S_{\theta\theta} - mS_{r\theta} \\
\rho dS_{r\theta}/d\rho &= -(2 + F(\rho))\, S_{r\theta} + mS_{\theta\theta} \\
\rho dw_r/d\rho &= S_{rr} - \nu S_{\theta\theta} - w_r \\
\rho dw_\theta/d\rho &= 2(1 + \nu)S_{r\theta} + mw_r \\
S_{\theta\theta} &= mw_\theta + w_r + \nu S_{rr}
\end{aligned} \tag{20}$$

where

$$F(\rho) \equiv \frac{r}{t}\frac{dt}{dr}$$

In the region $\rho \geq 1$ where the thickness of the plate is constant,

$$F(\rho) = 0 \tag{21}$$

while in the region $\rho \leq 1$ where the thickness of the plate varies

$$F(\rho) = \frac{2(1 - q)\,\rho^2}{q + (1 - q)\rho^2} \tag{22}$$

Expressions (18) show that only the cases $m = 0$ and $m = 2$ need be considered in order to satisfy boundary conditions at infinity. For $m = 0$ the boundary conditions

at infinity are, from (18) and (19)

$$S_{rr} \to 1/2, \qquad S_{\theta\theta} \to 1/2, \qquad S_{r\theta} \to 0 \tag{23}$$

while for m = 2 they are

$$S_{rr} \to 1/2, \qquad S_{\theta\theta} \to -1/2, \qquad S_{r\theta} \to -1/2 \tag{24}$$

The superposition of the solutions for m = 0 and m = 2 then satisfies (18) as well as the governing equations (16) and thus constitutes the solution to our problem.

In view of the different form of $F(\rho)$ in the two regions $\rho \leq 1$ and $\rho \geq 1$ (cf. (21) and (22)) the two regions must be considered separately. The procedure is to obtain solutions of equations (20) for each of the two regions and then adjust the constants of integration so that the two solutions match at $\rho = 1$.

Consider first the region $\rho \geq 1$. Here equations (20) are the governing equations for a plate of uniform thickness, the general solutions of which are known (Ref. 8). When specialized so as to satisfy the boundary conditions (23) or (24) the solutions of (20) are:

$$\text{for } m = 0, \quad \begin{aligned} S_{rr} &= 1/2 + K_o/\rho^2 \\ S_{\theta\theta} &= 1/2 - K_o/\rho^2 \\ w_r &= (1 - \nu)/2 - (1 + \nu)K_o/\rho^2 \\ w_\theta &= S_{r\theta} = 0 \end{aligned} \tag{25}$$

and for m = 2,

$$
\begin{aligned}
S_{rr} &= 1/2 - 2K_1/\rho^2 - 3K_2/\rho^4 \\
S_{\theta\theta} &= -1/2 + 3K_2/\rho^4 \\
S_{r\theta} &= -1/2 - K_1/\rho^2 - 3K_2/\rho^4 \\
w_r &= (1+\nu)/2 + 2K_1/\rho^2 + (1+\nu)K_2/\rho^4 \\
w_\theta &= -(1+\nu)/2 - (1-\nu)K_1/\rho^2 + (1+\nu)K_2/\rho^4
\end{aligned}
\tag{26}
$$

where K_o, K_1, K_2, are constants of integration.

Consider next the region $\rho \leq 1$ where $F(\rho)$ is given by (22). The solution of (20) for this region is more difficult than for the region $\rho \geq 1$. By use of the last equation of (20) $S_{\theta\theta}$ can be eliminated from the first four equations of (20), thus yielding the set of four ordinary linear differential equations

$$
\begin{aligned}
\rho dS_{rr}/d\rho &= (-1+\nu-F(\rho))S_{rr} - mS_{r\theta} + w_r + mw_\theta \\
\rho dS_{r\theta}/d\rho &= \nu mS_{rr} + (-2-F(\rho))S_{r\theta} + mw_r + m^2w_\theta \\
\rho dw_r/d\rho &= (1-\nu^2)S_{rr} - (1+\nu)w_r - \nu mw_\theta \\
\rho dw_\theta/d\rho &= 2(1+\nu)S_{r\theta} + mw_r
\end{aligned}
\tag{27}
$$

or, in matrix form

$$\rho dS/d\rho = (A_m - BF(\rho))S \tag{28}$$

where

$$S = \begin{pmatrix} S_{rr} \\ S_{r\theta} \\ w_r \\ w_\theta \end{pmatrix} \qquad A_m = \begin{pmatrix} -1+\nu & -m & 1 & m \\ \nu m & -2 & m & m^2 \\ 1-\nu^2 & 0 & -1-\nu & -\nu m \\ 0 & 2(1+\nu) & m & 0 \end{pmatrix} \tag{29}$$

$$B = \begin{pmatrix} 1 & 0 & 0 & 0 \\ 0 & 1 & 0 & 0 \\ 0 & 0 & 0 & 0 \\ 0 & 0 & 0 & 0 \end{pmatrix}$$

In equations (28) the parameter q appears, through the function $F(\rho)$, only in the combination $(1-q)\rho^2/q$. It is therefore possible to eliminate q from the equations by introducing a new independent variable y where

$$y = \rho\sqrt{((1 - q)/q)} \tag{30}$$

With this substitution (28) becomes

$$ydS/dy = (A_m - 2By^2/(1 + y^2))S \tag{31}$$

The fact that y appears on the right-hand side of (31) only in

the combination $y^2/(1 + y^2)$ suggests a further change of independent variable,

$$x = y^2/(1 + y^2) \tag{32}$$

This final change of variable reduces equation (28) to

$$2x(1 - x)dS/dx = (A_m - 2Bx)S \tag{33}$$

From (30) and (32) the connection between x and ρ is

$$x = \frac{(1 - q)\rho^2}{q + (1 - q)\rho^2}, \qquad \rho = \sqrt{\left(\frac{q}{1 - q}\right)\left(\frac{x}{1 - x}\right)} \tag{34}$$

The solution of (33) can be obtained in series form by Frobenius's method (Ref. 1). We assume a solution of the form

$$S = x^{\lambda}(S_o + xS_1 + x^2S_2 + x^3S_3 + \ldots) \tag{35}$$

and determine λ, S_o, S_1, etc., so that (33) is satisfied. By substituting (35) into (33) and equating coefficients of like powers of x we obtain

$$2\lambda S_o = A_m S_o \tag{36}$$

$$2(\lambda+k)S_k - 2(\lambda+k-1)S_{k-1} = A_m S_k - 2BS_{k-1}, \quad k = 1, 2, 3, \ldots \tag{37}$$

Equation (36) shows that λ must be an eigenvalue of $A_m/2$ and S_o the corresponding eigenvector. The eigenvalues of $A_m/2$ are readily found to be

$$\lambda_1 = (m/2) - 1 \qquad \lambda_2 = m/2$$
$$\lambda_3 = -m/2 \qquad \lambda_4 = -(m/2) - 1 \tag{38}$$

Let us restrict attention now to the case $m = 2$. From (38) the eigenvalues of $A_2/2$ are $\lambda_1 = 0$, $\lambda_2 = 1$, $\lambda_3 = -1$, $\lambda_4 = -2$. The eigenvalues λ_3 and λ_4, being negative, lead to solutions which give non-zero displacements at $x = 0$ and are therefore inadmissible. The remaining eigenvalues λ_1 and λ_2 lead to acceptable series solutions of (33) which we denote respectively by

$$P(x) = P_o + xP_1 + x^2P_2 + x^3P_3 + \ldots$$
$$Q(x) = \quad xQ_1 + x^2Q_2 + x^3Q_3 + \ldots \tag{39}$$

where P_o must be the eigenvector of $A_2/2$ corresponding to λ_1 and Q_1 the eigenvector corresponding to λ_2. It is readily found that

$$P_o = \begin{pmatrix} 1 \\ -1 \\ 1+\nu \\ -1-\nu \end{pmatrix} \qquad Q_1 = \begin{pmatrix} 0 \\ 1 \\ -2\nu/3 \\ 1+\nu/3 \end{pmatrix} \tag{40}$$

By comparing (39) with (35) and recalling $\lambda_1 = 0$, $\lambda_2 = 1$, the

recurrence relations for the two solutions P(x), Q(x), may be obtained from (37). Thus

$$2kP_K - 2(k-1)P_{K-1} = A_2P_K - 2BP_{K-1}$$
$$2kQ_K - 2(k-1)Q_{K-1} = A_2Q_K - 2BQ_{K-1} \qquad (41)$$

The fact that P_K and Q_K satisfy the same recurrence relation simplifies the numerical work. From (41) it follows

$$P_K = (2kI - A_2)^{-1}\,(2(k-1)I - 2B)P_{K-1}$$
$$Q_K = (2kI - A_2)^{-1}\,(2(k-1)I - 2B)Q_{K-1} \qquad (42)$$

provided the matrix $(2kI - A_2)$ is non-singular. This is true when $k \geq 2$ but not when $k = 1$. The equation connecting P_1 and P_o therefore requires special examination. For $k = 1$ the first equation of (41) is

$$(2I - A_2)P_1 = -2BP_o \qquad (43)$$

where the determinant of $(2I - A_2)$ vanishes. However BP_o is such that the set of equations (43) is consistent and it may be solved to give

$$P_1 = \frac{1}{3+\nu}\begin{pmatrix} -3-\nu \\ 1-\nu \\ -1+\nu 2 \\ 0 \end{pmatrix} + CQ_1 \qquad (44)$$

where C is an arbitrary constant. The result (44) should not be surprising in view of the form (39) of the solutions P(x) and Q(x). There is no loss of generality in setting C = 0.

We now have expressions for P_0, P_1 and Q_1. P_2 and Q_2 may be computed in terms of P_1 and Q_1 using (42) and in turn P_3, Q_3, P_4, Q_4, etc., may be computed. This establishes the two solutions P(x) and Q(x) of equation (33) for the case m = 2. The complete solution of (33) for the case m = 2 then is

$$S(x) = C_1 P(x) + C_2 Q(x) \tag{45}$$

where C_1 and C_2 are constants.

For the case m = 2 the quantities S_{rr}, w_r, etc., are given by (26) in the region $\rho \geq 1$ and by (45) in the region $\rho \leq 1$. It remains only to determine the constants C_1, C_2, K_1, K_2 which appear in these expressions. Now the expressions (26) and (45) must match at $\rho = 1$. Specifically the requirements are that the values of S_{rr}, $S_{r\theta}$, w_r, w_θ at $\rho = 1$ given by (26) must be respectively equal to the values of S_{rr}, $S_{r\theta}$, w_r, w_θ at $x = 1-q$ (cf. (34)) given by (45). With the notation

$$P(x) = \begin{pmatrix} p_1(x) \\ p_2(x) \\ p_3(x) \\ p_4(x) \end{pmatrix} \qquad Q(x) = \begin{pmatrix} q_1(x) \\ q_2(x) \\ q_3(x) \\ q_4(x) \end{pmatrix} \tag{46}$$

these matching requirements lead to the set of equations

$$\begin{pmatrix} p_1(1-q) & q_1(1-q) & 2 & 3 \\ p_2(1-q) & q_2(1-q) & 1 & 3 \\ p_3(1-q) & q_3(1-q) & -2 & -1-\nu \\ p_4(1-q) & q_4(1-q) & 1-\nu & -1-\nu \end{pmatrix} \begin{pmatrix} C_1 \\ C_2 \\ K_1 \\ K_2 \end{pmatrix} = \frac{1}{2} \begin{pmatrix} 1 \\ -1 \\ 1+\nu \\ -1-\nu \end{pmatrix} \tag{47}$$

from which the values of C_1, C_2, K_1, K_2, follow. This completes the derivation of the solution for the case $m = 2$.

The derivation of the solution for the case $m = 0$ is similar. However, certain simplifications appear since this case represents axisymmetric distributions of stress. In particular $S_{r\theta} \equiv 0$ and $w_s \equiv 0$. From (38) the eigenvalues of $A_o/2$ are $\lambda_1 = \lambda_4 = -1$ and $\lambda_2 = \lambda_3 = 0$. As before the negative eigenvalues lead to inadmissible solutions. Corresponding to the double eigenvalue $\lambda_2 = \lambda_3 = 0$ there are two linearly independent eigenvectors which lead to two linearly independent solutions of (28). One of these is a trivial rigid-body rotation which can be dropped without loss. The remaining solution, derived in the same way as P(x) and Q(x), is

$$R(x) = R_o + xR_1 + x^2R_2 + x^3R_3 + \ldots. \tag{48}$$

where

$$R_o = \begin{pmatrix} 1 \\ 0 \\ 1-\nu \\ 0 \end{pmatrix} \tag{49}$$

and

$$R_K = (2kI - A_o)^{-1}(2(k-1)I - 2B)R_{K-1}, \qquad k = 1, 2, 3, \ldots \quad (50)$$

The complete solution of (28) for the case m = 0 then is

$$S(x) = C_o\, R(x) \quad (51)$$

where C_o is a constant.

For the case m = 0 the quantities S_{rr}, w_r, etc., are given by (51) in the region $\rho \leq 1$ and by (26) in the region $\rho \geq 1$. As in the case m = 2, the constants in these expressions must be determined so that the expressions match at $\rho = 1$. Note here that $S_{r\theta}$ and w_θ automatically match since both are identically zero. The requirements that S_{rr} and w_r match at $\rho = 1$ yield the set of equations for C_o and K_o

$$\begin{pmatrix} r_1(1-q) & -1 \\ r_3(1-q) & 1+\nu \end{pmatrix} \begin{pmatrix} C_o \\ K_o \end{pmatrix} = \frac{1}{2} \begin{pmatrix} 1 \\ 1-\nu \end{pmatrix} \quad (52)$$

where the notation

$$R(x) = \begin{pmatrix} r_1(x) \\ 0 \\ r_3(x) \\ 0 \end{pmatrix} \quad (53)$$

has been introduced. This completes the derivation of the solution for the case m = 0.

The question of convergence of the series (39) and (48) is easily settled. The radius of convergence of a power series extends to the nearest singularity, and the singular points in the complex plane of equations (28) are $x = 0$, $x = 1$, and $x = \infty$. Hence the series (39) and (48) converge uniformly and absolutely for $|x| < 1$.* In view of (34) this means that the series converge for all values of ρ and q in the ranges of interest, $0 \leq \rho \leq 1$ and $0 < q \leq 1$. The introduction of x as the independent variable instead of y has an important advantage with regard to convergence. If the equations (31) were solved by Frobenius's method the resulting power series in y would converge for $|y| < 1$ since the singular points of equations (31) are $y = 0$, $y = \pm i$ and $y = \infty$. From (30), $y < 1$ at all points in the range $0 \leq \rho \leq 1$ only if $q > 1/2$. Hence the series in y would converge only for a limited range of the parameter q. The change of independent variable from y to x significantly widens the range of q for which the analysis is valid.

As stated before, the superposition of the solutions for $m = 0$ and $m = 2$ furnishes the required solution of our stress analysis problem. The final formulas for the stresses can be put in the form

$$\begin{aligned} \sigma_{rr}/\sigma_o &= f_o(\rho) + f_2(\rho) \cos 2\theta \\ \sigma_{\theta\theta}/\sigma_o &= g_o(\rho) + g_2(\rho) \cos 2\theta \\ \sigma_{r\theta}/\sigma_o &= \qquad\quad h_2(\rho) \sin 2\theta \end{aligned} \tag{54}$$

---

* With regard to the speed of convergence, a study of the recurrence relations reveals that P_K and Q_K are of order $k^{-0.296}$ while R_K is of order $k^{-1.408}$ for large k.

where f_o, f_2, g_o, g_2, h_2 are given by the following expressions. In the region $\rho \geq 1$,

$$f_o = 1/2 + K_o/\rho^2 \qquad f_2 = 1/2 - 2K_1/\rho^2 - 3K_2/\rho^4$$

$$g_o = 1/2 - K_o/\rho^2 \qquad g_2 = -1/2 + 3K_2/\rho^4 \qquad (55)$$

$$h_2 = -1/2 - K_1/\rho^2 - 3K_2/\rho^4$$

while in the region $\rho \leq 1$,

$$f_o = C_o r_1(x) \qquad f_2 = C_1 p_1(x) + C_2 q_1(x)$$

$$g_o = C_o(\nu r_1(x) + r_3(x)) \qquad g_2 = C_1(\nu p_1 + p_3 + 2p_4) + C_2(\nu q_1 + q_3 + 2q_4) \qquad (56)$$

$$h_2 = C_1 p_2(x) + C_2 q_2(x)$$

where

$$x = \frac{(1-q)\rho^2}{q + (1-q)\rho^2}$$

5.2 Special Case q = 0

The case q = 0 requires special consideration since the substitution (30) is no longer admissible. Although the situation q = 0 is impossible to achieve in practice, it is useful to have data for this case as it represents a limiting value of q.

When q = 0 the analysis as far as equation (29) is unchanged but the work dealing with the solution of equation (28) must be revised. When q = 0, $F(\rho) = 2$, and equation (28) becomes

$$\rho dS/d\rho = D_m S \tag{57}$$

where

$$D_m = \begin{pmatrix} -3+\nu & -m & 1 & m \\ \nu m & -4 & m & m^2 \\ 1-\nu^2 & 0 & -1-\nu & -\nu m \\ 0 & 2(1+\nu) & m & 0 \end{pmatrix} \tag{58}$$

The solution of equations equivalent to (57) is given, among other results, in Reference 2. We present here a slightly different method of solution which is more in line with the analysis of the previous section.

Equation (57) is an Euler equation which has solutions of the form $S = X\rho^{\mu}$ where X is a constant vector. Substitution into (57) yields

$$(D_m - \mu I)X = 0 \tag{59}$$

Hence μ must be an eigenvalue of D_m and X the corresponding eigenvector. Normally, four linearly independent solutions of (57) can be obtained in this way. In the case m = 2, two of the four solutions must be rejected on the grounds that they yield non-zero displacements at $\rho = 0$, and the remaining

two solutions may be combined linearly to form the complete solution

$$S = C_1 X_1 \rho^{\mu_1} + C_2 X_2 \rho^{\mu_2} \tag{60}$$

The eigenvalues μ_1, μ_2, and the corresponding eigenvectors X_1, X_2, are found to be

$$\mu_1 = -2 + \sqrt{7-\nu + \sqrt{(7-\nu)^2 - 16(1+\nu)}}$$

$$\mu_2 = -2 + \sqrt{7-\nu - \sqrt{(7-\nu)^2 - 16(1+\nu)}} \tag{61}$$

$$X_i = \begin{pmatrix} \mu_i^3 + (5+\nu)\mu_i^2 - 4\mu_i - 8(1-\nu) \\ 2\nu\mu_i^2 + 2(1+\nu)\mu_i + 8 \\ (1-\nu^2)\mu_i^2 + 4(1-\nu^2)\mu_i - 8(1+\nu) \\ 2(1+\nu)^2\mu_i + 4(3-\nu)(1+\nu) \end{pmatrix} \quad i = 1, 2$$

In the case m = 0, two solutions must be rejected as before and one of the remaining two solutions is a trivial rigid-body rotation which can also be discarded. The remaining solution is

$$S = C_o X_o \rho^{\mu_o} \tag{62}$$

where $$\mu_o = -2 + \sqrt{2(1-\nu)}$$

and

$$X_o = \begin{pmatrix} 1 \\ 0 \\ 1-\nu + \sqrt{2(1-\nu)} \\ 0 \end{pmatrix} \qquad (63)$$

Expressions (60) and (62) are the appropriate solutions of (28) when $q = 0$. As such they replace expressions (45) and (51) respectively. With these replacements the remaining steps in the derivation of the solution when $q = 0$ are the same as in the previous section.

More details of the derivation of (60) and (62), in particular the procedure for obtaining the eigenvalues of D_m, can be found in Reference 2.

5.3 Numerical Work

It will be appreciated that the computational work is fairly lengthy, although not so lengthy as to be beyond the range of a desk calculator. Except for the calculation of P_K, Q_K, R_K, which was carried out on the Structures Laboratory's Ferranti electronic computer using a program prepared by Miss Helen Tulloch, all computations were done on a desk computer.

The procedure for computing $f_o(\rho)$, $f_2(\rho)$, etc. should be apparent from the analysis of the preceding sections. The procedure for computing the derivatives of these functions, however, requires some mention. For computing the derivatives values of $dP/d\rho$, $dQ/d\rho$, $dR/d\rho$ are needed, which may be obtained in one of the following ways. Consider, for example, $dP/d\rho$.

In view of (34),

$$\frac{dP}{d\rho} = \frac{2q(1-q)\rho}{(q + (1-q)\rho^2)^2} \frac{dP}{dx} \tag{64}$$

and from (39)

$$dP/dx = P_1 + 2xP_2 + 3x^2P_3 + 4x^3P_4 + \ldots \tag{65}$$

Thus $dP/d\rho$ may be obtained by summing the series (65) and using (64). Alternatively, since P satisfies (28), $dP/d\rho$ may be obtained from the formula

$$dP/d\rho = (A_2 - BF(\rho))P/\rho. \tag{66}$$

The latter method of calculation was used since it requires less work and since the convergence of (65) is poor when x is large. The fact that the right-hand side of (66) degenerates to the form 0/0 as ρ tends to zero causes no difficulty. In a few cases derivatives were calculated by both methods as a check.

At least five places of decimals were retained in the calculation of P_K, Q_K, R_K, and at least four places of decimals in the other steps of the computations. Twenty terms were retained in the power series summations and the remainder after twenty terms was estimated by approximating the remainder by a geometric series. In the worst case of convergence the error involved in this procedure is less than

0.03 percent. As a check on the numerical work several computations, including the computation of P_K, Q_K, R_K, were performed twice. A further check was provided by calculating some derivatives in two ways, as already mentioned. As a final check, a finite-difference formula was applied to a sampling of the tabulated values of f_o, f_2, etc., to obtain the derivatives of these functions which were then compared with the tabulated values of the derivatives. The final results quoted in the tables should be accurate to the number of figures given.

Although equations (42) and (50) may be used as they stand, a more convenient formula for computing P_K, Q_K, R_K, can be obtained. Consider, for example, the equation for P_K,

$$\begin{aligned}(2kI - A_2)P_K &= (2(k-1)I - 2B)P_{K-1} \\ &= (2kI - A_2)P_{K-1} + (A_2 - 2I - 2B)P_{K-1}\end{aligned} \tag{67}$$

Let M be the matrix of eigenvectors of A_2 and Λ the diagonal matrix of eigenvalues of A_2 so that $M^{-1}A_2M = \Lambda$. From (67) we obtain

$$\begin{aligned}M^{-1}(2kI - A_2)MM^{-1}P_K &= M^{-1}(2kI - A_2)MM^{-1}P_{K-1} \\ &\quad + M^{-1}(A_2 - 2I - 2B)P_{K-1}\end{aligned} \tag{68}$$

or $\quad (2kI - \Lambda)M^{-1}P_K = (2kI - \Lambda)M^{-1}P_{K-1} + M^{-1}(A_2 - 2I - 2B)P_{K-1}$

Now $(2kI - \Lambda)$ is a diagonal matrix and is easily invertible. Solving (68) for P_K gives

$$P_K = P_{K-1} + M(2kI - \Lambda)^{-1}M^{-1}(A_2 - 2I - 2B)P_{K-1}$$

or, with a change in notation

$$P_K = P_{K-1} + MN_{K-1}LP_{K-1} \tag{69}$$

where $N_{K-1} \equiv 2(2kI - \Lambda)^{-1}$ and $L \equiv M^{-1}(A_2 - 2I - 2B)/2$. The evaluation of M, Λ, N_K, and L, is straightforward and we find

$$L = \begin{pmatrix} -(1+\nu)/3 & -(1+\nu)/3 & 0 & 0 \\ -2 & (1-\nu) & -1 & -1/2 \\ -3(1+\nu)/2 & 3(1+\nu)/2 & 1 & -1 \\ 2\nu & -(3+\nu) & 0 & 9/4 \end{pmatrix}$$

$$N_K = \begin{pmatrix} 1/k & 0 & 0 & 0 \\ 0 & 1/(k+1) & 0 & 0 \\ 0 & 0 & 1/(k+2) & 0 \\ 0 & 0 & 0 & 1/(k+3) \end{pmatrix}$$

$$M = \begin{pmatrix} 0 & 1/2 & 1 & 1 \\ 3/4 & -1/2 & 1/2 & 1 \\ -\nu/2 & (1+\nu)/2 & -1 & -(1+\nu)/3 \\ (3+\nu)/4 & -(1+\nu)/2 & (1-\nu)/2 & -(1+\nu)/3 \end{pmatrix}$$

Formula (69) is well suited to computation. It has the advantage of requiring no matrix inversion, and in addition the matrices M and L are constant while N_K varies with k only in a very simple way. Formula (69) also applies to Q_K and a similar formula can be derived for R_K.

6.0 REFERENCES

1. Burkill, J.C. — The Theory of Ordinary Differential Equations, pp. 36-39. Oliver and Boyd, London, 1956. Interscience Publishers Inc., N.Y.

2. Conway, H.D. — Analysis of Plane Stress in Polar Co-ordinates and with Varying Thickness. Transactions of the ASME, Series E - J. Appl. Mech., Vol. 26, No. 3, September 1959, pp. 437-439.

3. Green, A.E. Zerna, W. — Theoretical Elasticity, p. 260 and pp. 370-374. Oxford, Clarendon Press, 1954.

4. Timoshenko, S.P. Goodier, J.N. — Theory of Elasticity, 2nd ed. pp. 65-66. McGraw-Hill, New York, 1951.

5. Ibid. pp. 46-49, especially p. 49.

6. Ibid. pp. 96-98.

7. Ibid. pp. 241-244.

8. Ibid. p. 116.

/AM

TABLE IV

VALUES OF f_o $\nu = 0.3$

ρ \ q	1.0	0.8	0.6	0.4	0.2	0
0	0.500	0.576	0.687	0.867	1.250	∞
0.1	0.500	0.575	0.683	0.857	1.210	2.060
0.2	0.500	0.572	0.672	0.827	1.107	1.170
0.3	0.500	0.566	0.655	0.782	0.975	0.840
0.4	0.500	0.558	0.632	0.728	0.842	0.664
0.5	0.500	0.548	0.606	0.671	0.725	0.554
0.6	0.500	0.537	0.577	0.614	0.627	0.477
0.7	0.500	0.524	0.547	0.560	0.547	0.420
0.8	0.500	0.511	0.516	0.511	0.482	0.377
0.9	0.500	0.496	0.486	0.467	0.429	0.342
1.0	0.500	0.481	0.457	0.427	0.386	0.314
1.1	0.500	0.484	0.465	0.440	0.406	0.347
1.2	0.500	0.487	0.470	0.450	0.421	0.371
1.3	0.500	0.489	0.475	0.457	0.433	0.390
1.4	0.500	0.490	0.478	0.463	0.442	0.405
1.5	0.500	0.492	0.481	0.468	0.449	0.418
1.6	0.500	0.493	0.483	0.472	0.456	0.428
1.7	0.500	0.494	0.485	0.475	0.461	0.436
1.8	0.500	0.494	0.487	0.478	0.465	0.443
1.9	0.500	0.495	0.488	0.480	0.468	0.449
2.0	0.500	0.495	0.489	0.482	0.472	0.454

Table V
LR-340

TABLE V

VALUES OF g_o $\nu = 0.3$

ρ \ q	1.0	0.8	0.6	0.4	0.2	0
0	0.500	0.576	0.687	0.867	1.250	∞
0.1	0.500	0.576	0.685	0.861	1.227	4.498
0.2	0.500	0.574	0.679	0.844	1.165	2.554
0.3	0.500	0.570	0.668	0.817	1.083	1.834
0.4	0.500	0.566	0.655	0.784	0.995	1.450
0.5	0.500	0.560	0.639	0.748	0.910	1.208
0.6	0.500	0.553	0.621	0.710	0.834	1.041
0.7	0.500	0.546	0.602	0.673	0.767	0.918
0.8	0.500	0.538	0.582	0.637	0.709	0.823
0.9	0.500	0.529	0.562	0.604	0.658	0.748
1.0	0.500	0.519	0.543	0.573	0.614	0.686
1.1	0.500	0.516	0.535	0.560	0.594	0.654
1.2	0.500	0.513	0.530	0.551	0.579	0.629
1.3	0.500	0.511	0.525	0.543	0.567	0.610
1.4	0.500	0.510	0.522	0.537	0.558	0.595
1.5	0.500	0.509	0.519	0.532	0.551	0.583
1.6	0.500	0.508	0.517	0.528	0.545	0.573
1.7	0.500	0.506	0.515	0.525	0.539	0.564
1.8	0.500	0.506	0.513	0.522	0.535	0.557
1.9	0.500	0.505	0.512	0.520	0.532	0.551
2.0	0.500	0.505	0.511	0.518	0.529	0.546

TABLE VI

VALUES OF $df_c/d\rho$ $\quad \nu = 0.3$

ρ \ q	1.0	0.8	0.6	0.4	0.2	0
0	0	0	0	0	0	$-\infty$
0.1	0	-0.024	-0.073	-0.209	-0.764	-16.83
0.2	0	-0.047	-0.144	-0.383	-1.235	-4.777
0.3	0	-0.068	-0.202	-0.503	-1.360	-2.287
0.4	0	-0.088	-0.248	-0.565	-1.263	-1.356
0.5	0	-0.106	-0.280	-0.578	-1.080	-0.904
0.6	0	-0.121	-0.298	-0.557	-0.888	-0.649
0.7	0	-0.133	-0.305	-0.516	-0.720	-0.491
0.8	0	-0.142	-0.303	-0.467	-0.582	-0.385
0.9	0	-0.149	-0.294	-0.416	-0.475	-0.311
1.0-	0	-0.154	-0.281	-0.368	-0.390	-0.257
1.0+	0	0.038	0.085	0.145	0.228	0.372
1.1	0	0.029	0.064	0.109	0.171	0.279
1.2	0	0.022	0.049	0.084	0.132	0.215
1.3	0	0.018	0.039	0.066	0.104	0.169
1.4	0	0.014	0.031	0.053	0.083	0.136
1.5	0	0.011	0.025	0.043	0.068	0.110
1.6	0	0.009	0.021	0.036	0.056	0.091
1.7	0	0.008	0.017	0.030	0.046	0.076
1.8	0	0.007	0.015	0.025	0.039	0.064
1.9	0	0.006	0.012	0.021	0.033	0.054
2.0	0	0.005	0.011	0.018	0.029	0.046

TABLE VII

VALUES OF $dg_o/d\rho$ $\nu = 0.3$

ρ \ q	1.0	0.8	0.6	0.4	0.2	0
0	0	0	0	0	0	- ∞
0.1	0	-0.014	-0.043	-0.121	-0.446	-36.74
0.2	0	-0.027	-0.083	-0.225	-0.750	-10.43
0.3	0	-0.040	-0.119	-0.303	-0.876	-4.992
0.4	0	-0.051	-0.148	-0.351	-0.873	-2.960
0.5	0	-0.062	-0.170	-0.373	-0.805	-1.974
0.6	0	-0.072	-0.186	-0.376	-0.715	-1.417
0.7	0	-0.079	-0.195	-0.365	-0.625	-1.071
0.8	0	-0.087	-0.199	-0.346	-0.544	-0.840
0.9	0	-0.091	-0.199	-0.323	-0.473	-0.678
1.0-	0	-0.096	-0.196	-0.299	-0.413	-0.560
1.0+	0	-0.038	-0.085	-0.145	-0.228	-0.372
1.1	0	-0.029	-0.064	-0.109	-0.171	-0.279
1.2	0	-0.022	-0.049	-0.084	-0.132	-0.215
1.3	0	-0.018	-0.039	-0.066	-0.104	-0.169
1.4	0	-0.014	-0.031	-0.053	-0.083	-0.136
1.5	0	-0.011	-0.025	-0.043	-0.068	-0.110
1.6	0	-0.009	-0.021	-0.036	-0.056	-0.091
1.7	0	-0.008	-0.017	-0.030	-0.046	-0.076
1.8	0	-0.007	-0.015	-0.025	-0.039	-0.064
1.9	0	-0.006	-0.012	-0.021	-0.033	-0.054
2.0	0	-0.005	-0.011	-0.018	-0.029	-0.046

TABLE VIII

VALUES OF f_2 $\nu = 0.3$

ρ \ q	1.0	0.8	0.6	0.4	0.2	0
0	0.500	0.579	0.691	0.870	1.230	∞
0.1	0.500	0.578	0.687	0.857	1.182	0.424
0.2	0.500	0.573	0.674	0.821	1.060	0.270
0.3	0.500	0.566	0.652	0.767	0.905	0.208
0.4	0.500	0.557	0.625	0.702	0.753	0.174
0.5	0.500	0.545	0.593	0.634	0.621	0.153
0.6	0.500	0.531	0.558	0.567	0.513	0.138
0.7	0.500	0.516	0.522	0.505	0.428	0.127
0.8	0.500	0.499	0.486	0.449	0.361	0.120
0.9	0.500	0.482	0.451	0.399	0.309	0.114
1.0	0.500	0.464	0.418	0.356	0.268	0.110
1.1	0.500	0.465	0.421	0.363	0.280	0.134
1.2	0.500	0.467	0.426	0.373	0.297	0.165
1.3	0.500	0.470	0.433	0.384	0.315	0.197
1.4	0.500	0.473	0.439	0.394	0.333	0.226
1.5	0.500	0.475	0.444	0.404	0.348	0.253
1.6	0.500	0.477	0.449	0.413	0.363	0.276
1.7	0.500	0.480	0.454	0.421	0.375	0.297
1.8	0.500	0.481	0.458	0.428	0.386	0.316
1.9	0.500	0.483	0.462	0.434	0.396	0.332
2.0	0.500	0.484	0.465	0.440	0.405	0.346

TABLE IX

VALUES OF g_2 $\nu = 0.3$

ρ \ q	1.0	0.8	0.6	0.4	0.2	0
0	-0.500	-0.579	-0.691	-0.870	-1.230	$-\infty$
0.1	-0.500	-0.579	-0.690	-0.867	-1.222	-4.990
0.2	-0.500	-0.577	-0.687	-0.859	-1.197	-3.132
0.3	-0.500	-0.575	-0.681	-0.845	-1.157	-2.365
0.4	-0.500	-0.572	-0.672	-0.826	-1.103	-1.919
0.5	-0.500	-0.568	-0.661	-0.801	-1.040	-1.615
0.6	-0.500	-0.563	-0.648	-0.772	-0.972	-1.387
0.7	-0.500	-0.557	-0.633	-0.740	-0.903	-1.204
0.8	-0.500	-0.551	-0.616	-0.705	-0.833	-1.051
0.9	-0.500	-0.543	-0.598	-0.668	-0.764	-0.918
1.0	-0.500	-0.535	-0.577	-0.629	-0.698	-0.799
1.1	-0.500	-0.524	-0.553	-0.588	-0.635	-0.704
1.2	-0.500	-0.517	-0.537	-0.562	-0.595	-0.644
1.3	-0.500	-0.512	-0.527	-0.545	-0.569	-0.605
1.4	-0.500	-0.509	-0.520	-0.534	-0.551	-0.578
1.5	-0.500	-0.507	-0.515	-0.526	-0.539	-0.559
1.6	-0.500	-0.505	-0.512	-0.520	-0.530	-0.546
1.7	-0.500	-0.504	-0.509	-0.516	-0.524	-0.536
1.8	-0.500	-0.503	-0.507	-0.512	-0.519	-0.529
1.9	-0.500	-0.503	-0.506	-0.510	-0.515	-0.523
2.0	-0.500	-0.502	-0.505	-0.508	-0.512	-0.519

TABLE X

VALUES OF h_2 $\nu = 0.3$

ρ \ q	1.0	0.8	0.6	0.4	0.2	0
0	-0.500	-0.579	-0.691	-0.870	-1.230	$-\infty$
0.1	-0.500	-0.578	-0.689	-0.862	-1.202	-2.992
0.2	-0.500	-0.575	-0.680	-0.840	-1.130	-1.883
0.3	-0.500	-0.571	-0.667	-0.806	-1.034	-1.429
0.4	-0.500	-0.564	-0.649	-0.765	-0.934	-1.168
0.5	-0.500	-0.557	-0.628	-0.720	-0.841	-0.993
0.6	-0.500	-0.547	-0.604	-0.674	-0.758	-0.863
0.7	-0.500	-0.537	-0.579	-0.629	-0.685	-0.762
0.8	-0.500	-0.526	-0.554	-0.585	-0.622	-0.679
0.9	-0.500	-0.513	-0.528	-0.545	-0.567	-0.608
1.0	-0.500	-0.501	-0.503	-0.507	-0.517	-0.546
1.1	-0.500	-0.506	-0.513	-0.525	-0.543	-0.581
1.2	-0.500	-0.508	-0.518	-0.532	-0.554	-0.595
1.3	-0.500	-0.509	-0.520	-0.536	-0.558	-0.599
1.4	-0.500	-0.509	-0.521	-0.536	-0.558	-0.598
1.5	-0.500	-0.509	-0.520	-0.535	-0.556	-0.594
1.6	-0.500	-0.509	-0.519	-0.534	-0.554	-0.589
1.7	-0.500	-0.508	-0.518	-0.532	-0.551	-0.584
1.8	-0.500	-0.508	-0.517	-0.530	-0.547	-0.578
1.9	-0.500	-0.507	-0.516	-0.528	-0.544	-0.573
2.0	-0.500	-0.507	-0.515	-0.526	-0.541	-0.568

TABLE XI

VALUES OF df_2/dp $\nu = 0.3$

p \ q	1.0	0.8	0.6	0.4	0.2	0
0	0	0	0	0	0	$-\infty$
0.1	0	-0.029	-0.091	-0.253	-0.901	-2.793
0.2	0	-0.057	-0.175	-0.464	-1.456	-0.873
0.3	0	-0.083	-0.246	-0.605	-1.581	-0.437
0.4	0	-0.107	-0.300	-0.674	-1.440	-0.263
0.5	0	-0.128	-0.337	-0.682	-1.200	-0.175
0.6	0	-0.146	-0.357	-0.650	-0.959	-0.123
0.7	0	-0.160	-0.362	-0.594	-0.752	-0.090
0.8	0	-0.171	-0.357	-0.528	-0.587	-0.066
0.9	0	-0.179	-0.343	-0.461	-0.459	-0.050
1.0-	0	-0.183	-0.324	-0.399	-0.361	-0.037
1.0+	0	0.002	0.010	0.029	0.069	0.182
1.1	0	0.020	0.048	0.089	0.154	0.293
1.2	0	0.026	0.061	0.108	0.179	0.317
1.3	0	0.027	0.062	0.109	0.178	0.305
1.4	0	0.026	0.059	0.103	0.166	0.280
1.5	0	0.024	0.054	0.094	0.150	0.251
1.6	0	0.022	0.049	0.084	0.134	0.223
1.7	0	0.019	0.043	0.075	0.119	0.196
1.8	0	0.017	0.038	0.066	0.105	0.173
1.9	0	0.015	0.034	0.059	0.093	0.153
2.0	0	0.014	0.030	0.052	0.083	0.135

TABLE XII

VALUES OF $dg_2/d\rho$ $\nu = 0.3$

ρ \ q	1.0	0.8	0.6	0.4	0.2	0
0	0	0	0	0	0	∞
0.1	0	0.009	0.024	0.056	0.143	33.24
0.2	0	0.018	0.048	0.112	0.325	10.67
0.3	0	0.027	0.072	0.168	0.477	5.583
0.4	0	0.035	0.096	0.221	0.591	3.588
0.5	0	0.044	0.119	0.268	0.660	2.591
0.6	0	0.053	0.141	0.308	0.693	2.018
0.7	0	0.061	0.161	0.339	0.701	1.659
0.8	0	0.070	0.179	0.362	0.693	1.419
0.9	0	0.078	0.195	0.378	0.678	1.252
1.0-	0	0.085	0.209	0.389	0.659	1.131
1.0+	0	0.141	0.309	0.517	0.789	1.197
1.1	0	0.088	0.192	0.321	0.490	0.743
1.2	0	0.057	0.124	0.208	0.317	0.481
1.3	0	0.038	0.083	0.139	0.213	0.322
1.4	0	0.026	0.058	0.096	0.147	0.223
1.5	0	0.019	0.041	0.068	0.104	0.158
1.6	0	0.013	0.030	0.049	0.075	0.114
1.7	0	0.010	0.022	0.036	0.056	0.084
1.8	0	0.008	0.016	0.027	0.042	0.063
1.9	0	0.006	0.013	0.021	0.032	0.048
2.0	0	0.004	0.010	0.016	0.025	0.037

TABLE XIII

VALUES OF dh_2/dp $\nu = 0.3$

p \ q	1.0	0.8	0.6	0.4	0.2	0
0	0	0	0	0	0	∞
0.1	0	0.018	0.058	0.154	0.541	19.88
0.2	0	0.037	0.111	0.286	0.879	6.343
0.3	0	0.055	0.158	0.382	1.003	3.287
0.4	0	0.071	0.196	0.438	0.976	2.085
0.5	0	0.085	0.224	0.461	0.883	1.481
0.6	0	0.098	0.243	0.459	0.775	1.133
0.7	0	0.109	0.254	0.443	0.676	0.913
0.8	0	0.118	0.258	0.419	0.592	0.765
0.9	0	0.125	0.257	0.391	0.523	0.660
1.0-	0	0.131	0.253	0.364	0.467	0.584
1.0+	0	-0.069	-0.150	-0.244	-0.360	-0.507
1.1	0	-0.034	-0.072	-0.116	-0.168	-0.225
1.2	0	-0.015	-0.032	-0.050	-0.069	-0.082
1.3	0	-0.005	-0.011	-0.015	-0.017	-0.009
1.4	0	0	0.001	0.003	0.010	0.029
1.5	0	0.003	0.007	0.013	0.023	0.047
1.6	0	0.004	0.010	0.017	0.029	0.054
1.7	0	0.005	0.011	0.019	0.032	0.056
1.8	0	0.005	0.011	0.019	0.032	0.055
1.9	0	0.005	0.011	0.019	0.031	0.052
2.0	0	0.005	0.010	0.018	0.029	0.049

FIG. 1
LR-340

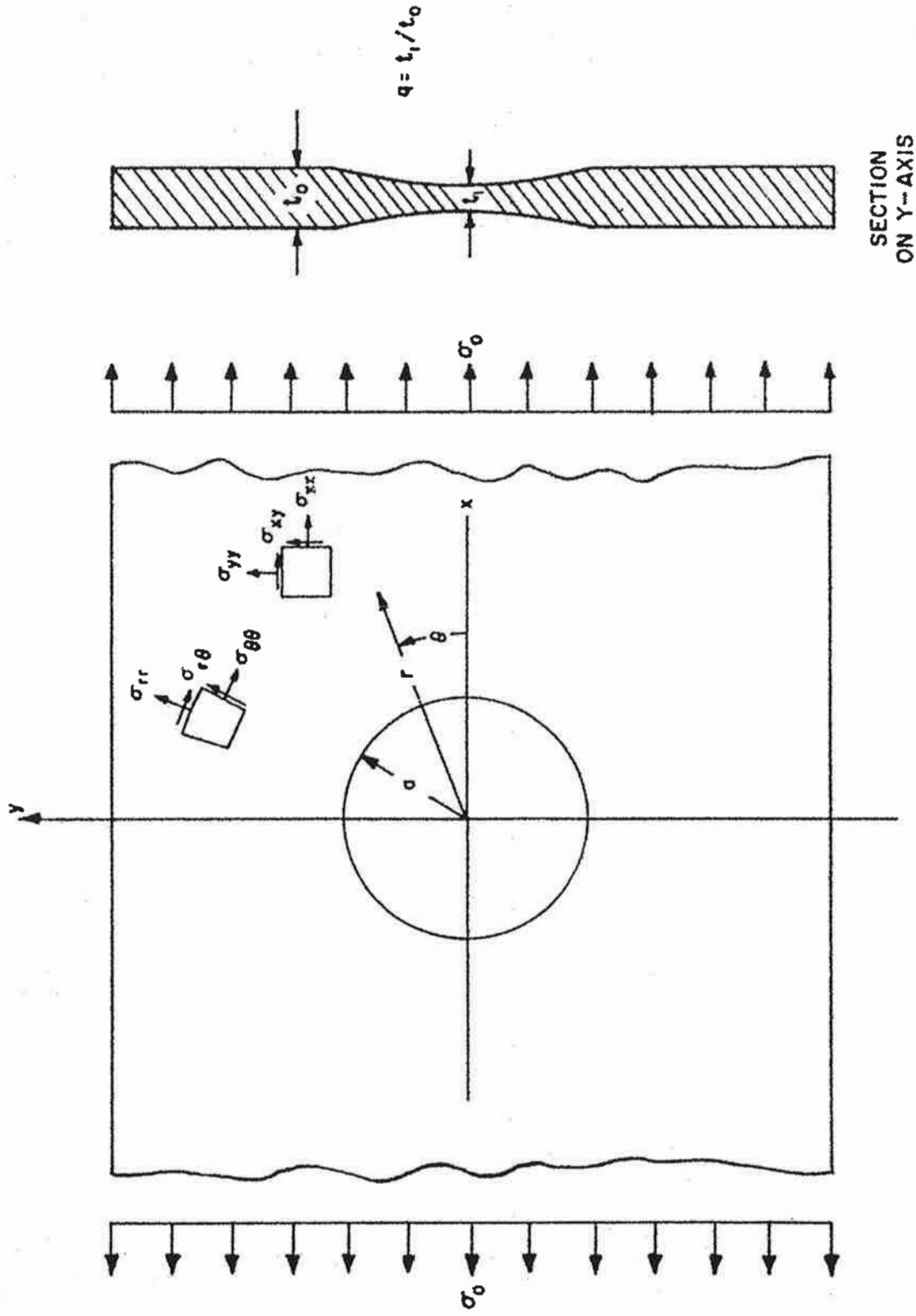

GEOMETRY OF PLATE

FIG. 2
LR-340

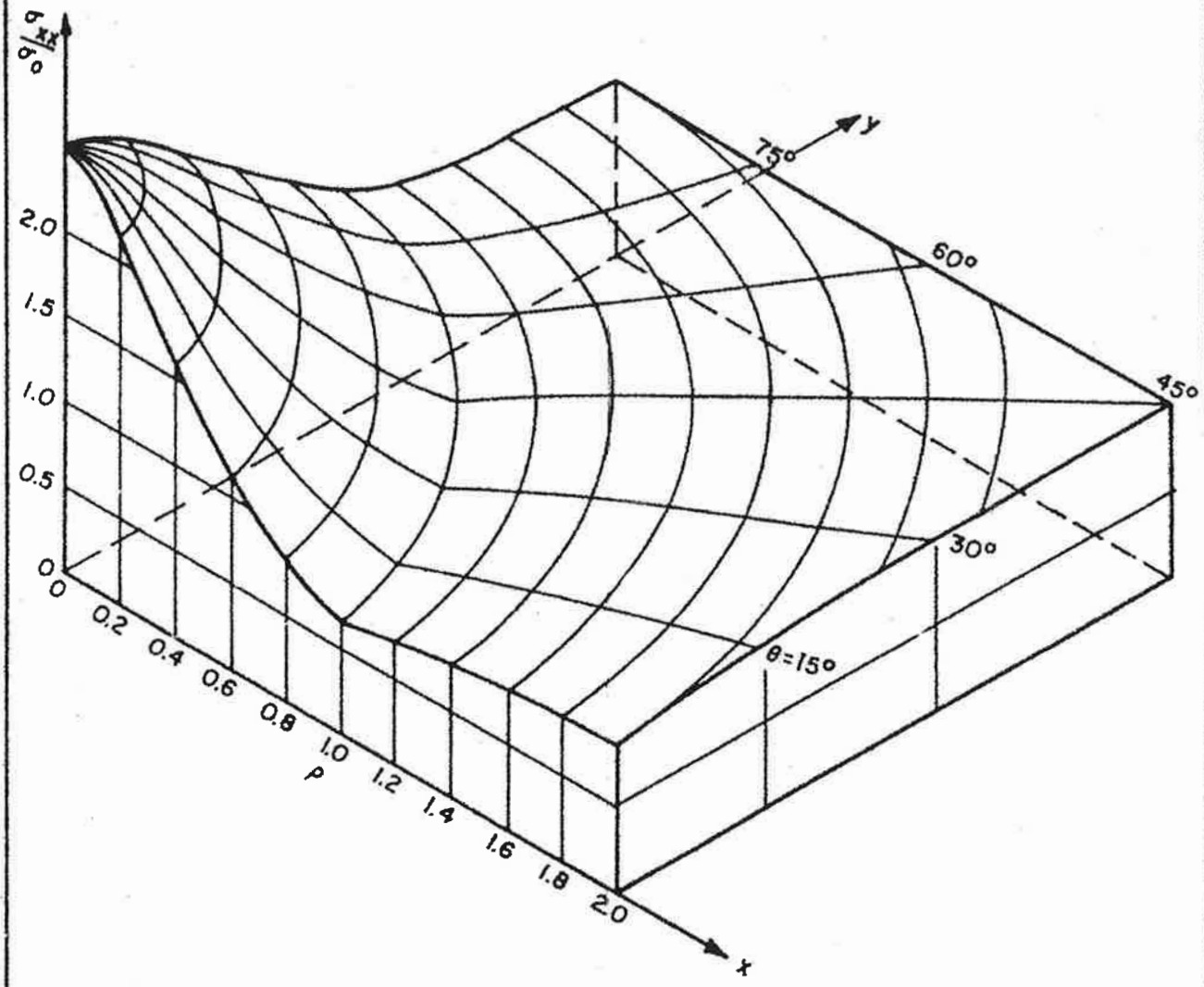

DISTRIBUTION OF STRESS σ_{xx}, q=0.2

FIG. 3a, b
LR-340

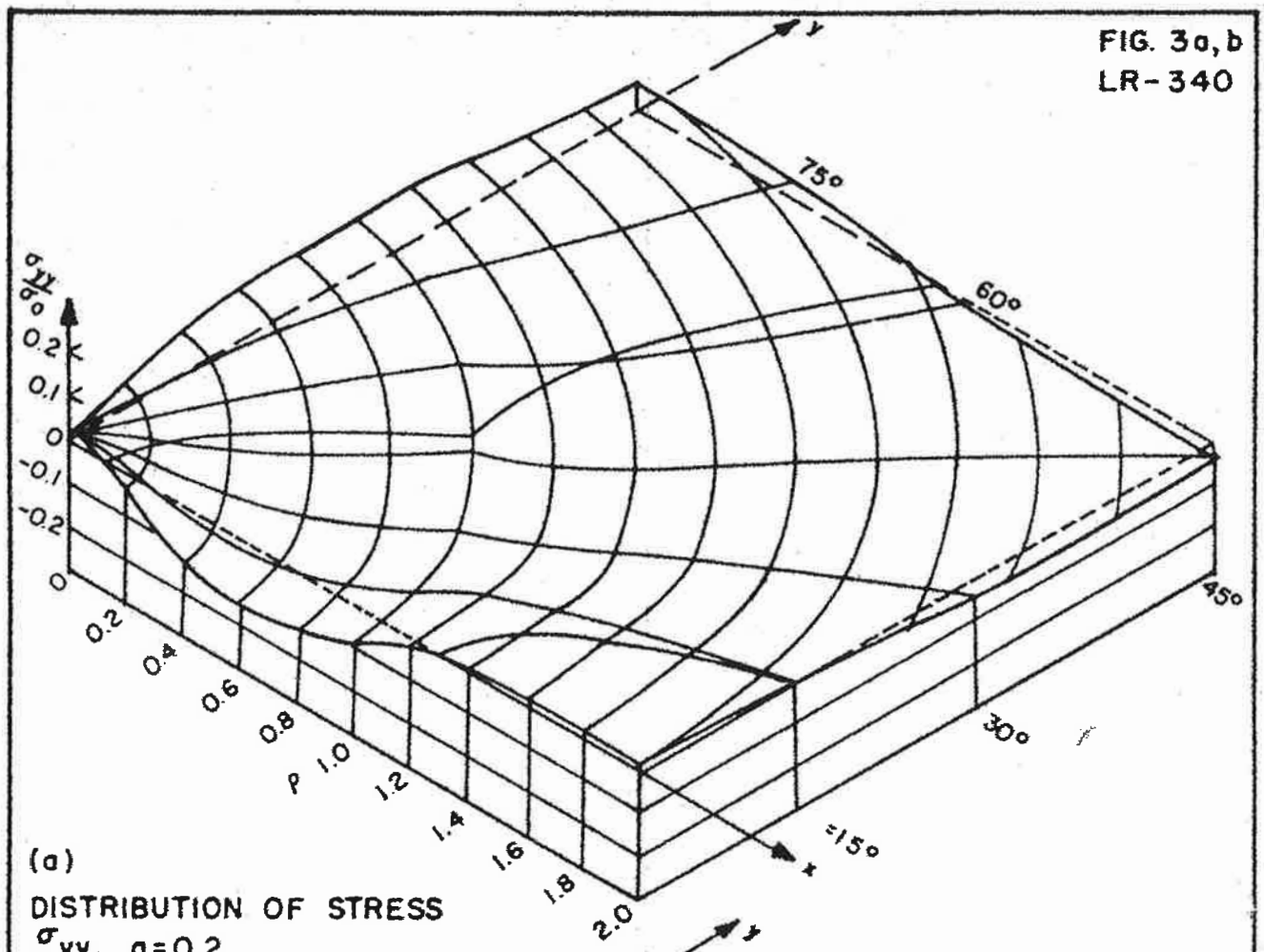

(a)
DISTRIBUTION OF STRESS
σ_{yy}, q=0.2

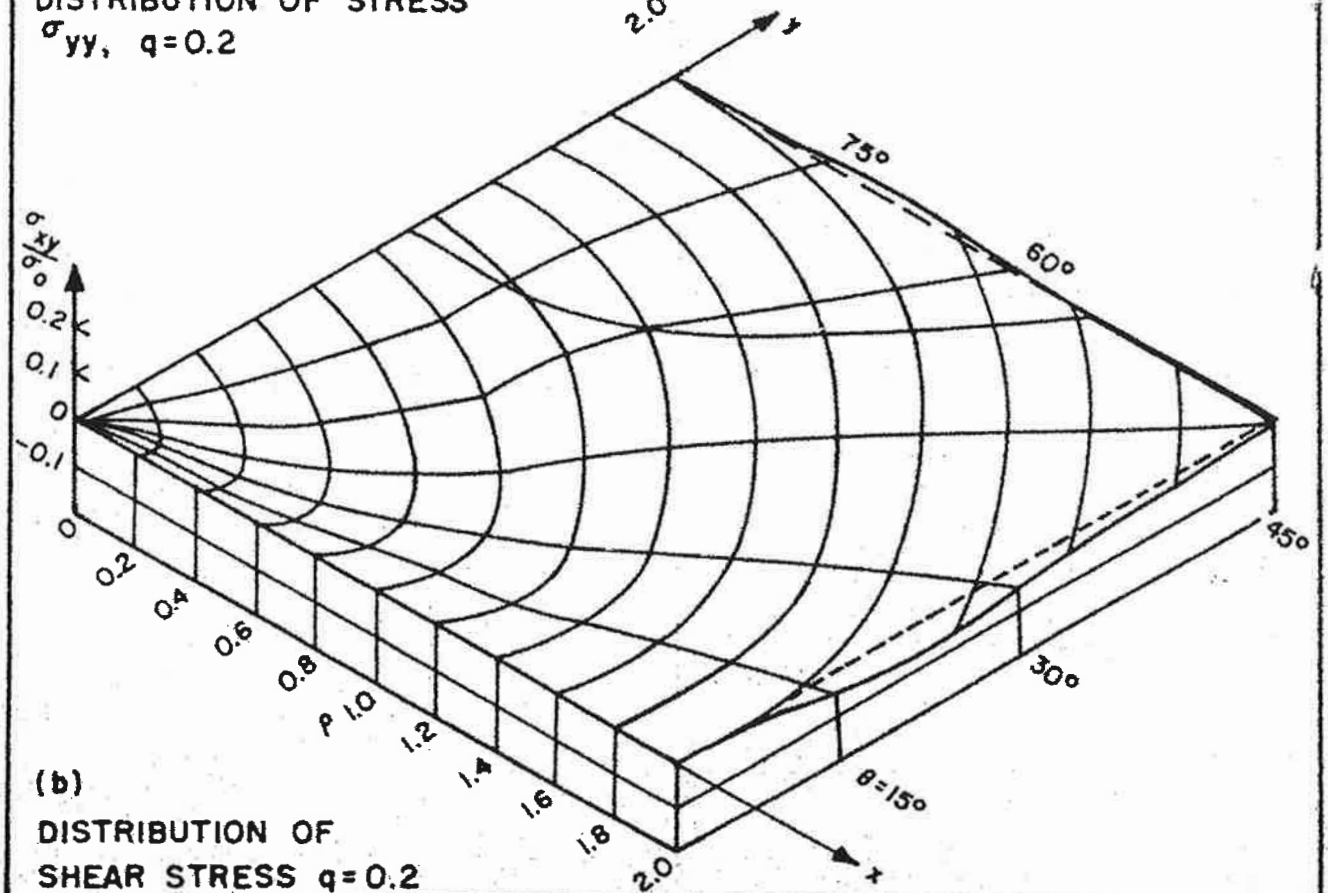

(b)
DISTRIBUTION OF
SHEAR STRESS q=0.2

FIG. 4
LR-340

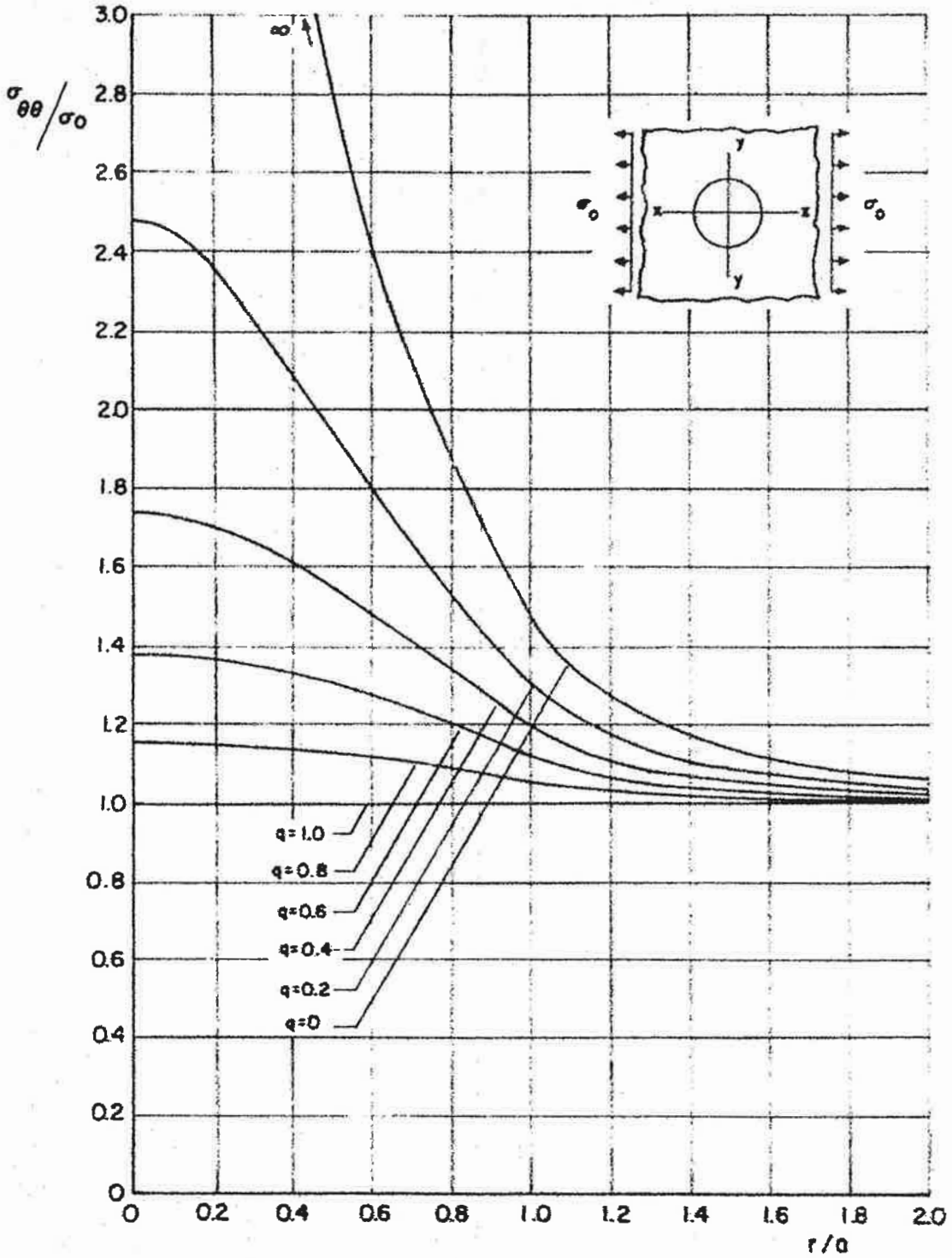

TANGENTIAL STRESS ON Y-Y

FIG. 5
LR-340

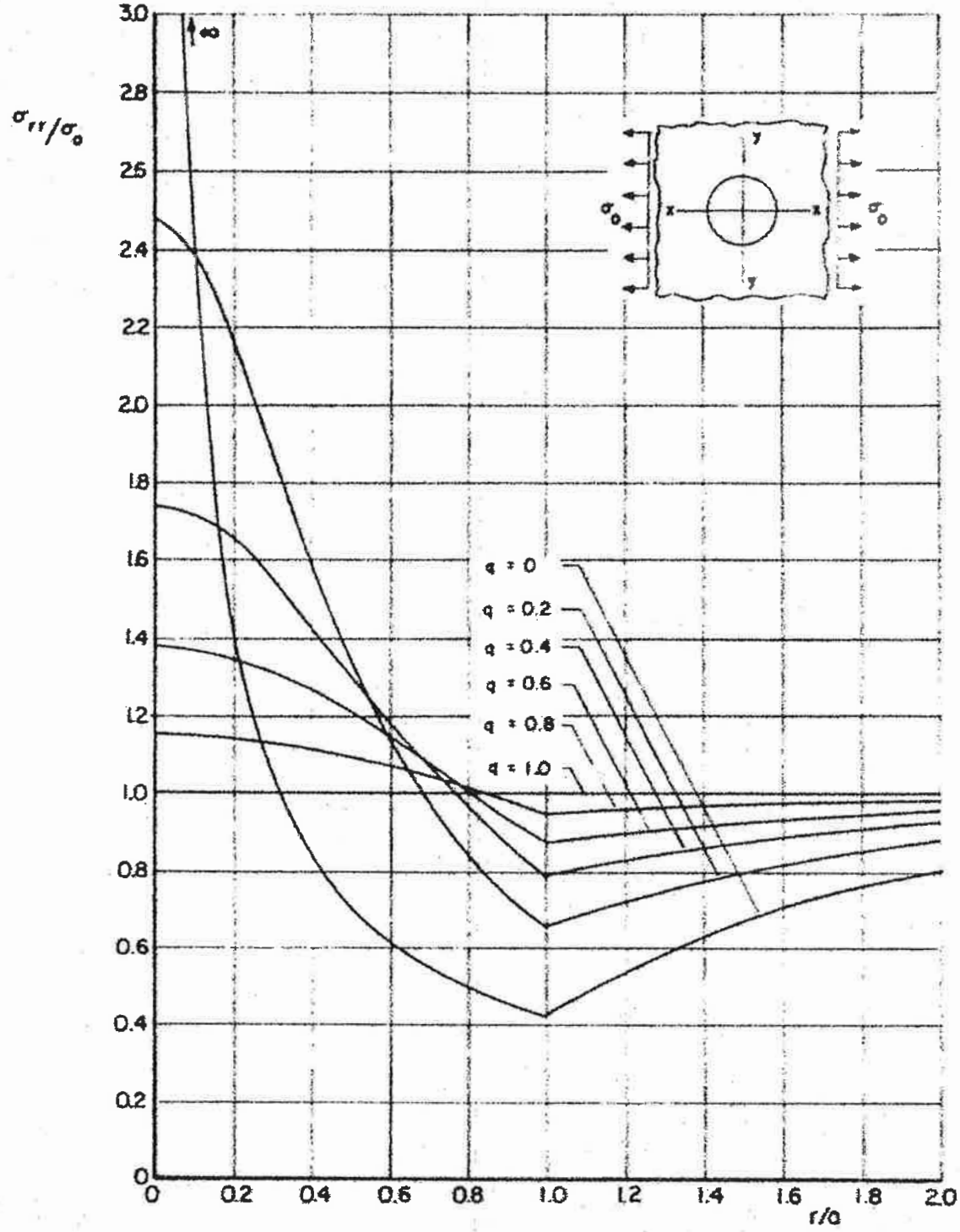

RADIAL STRESS ON X-X

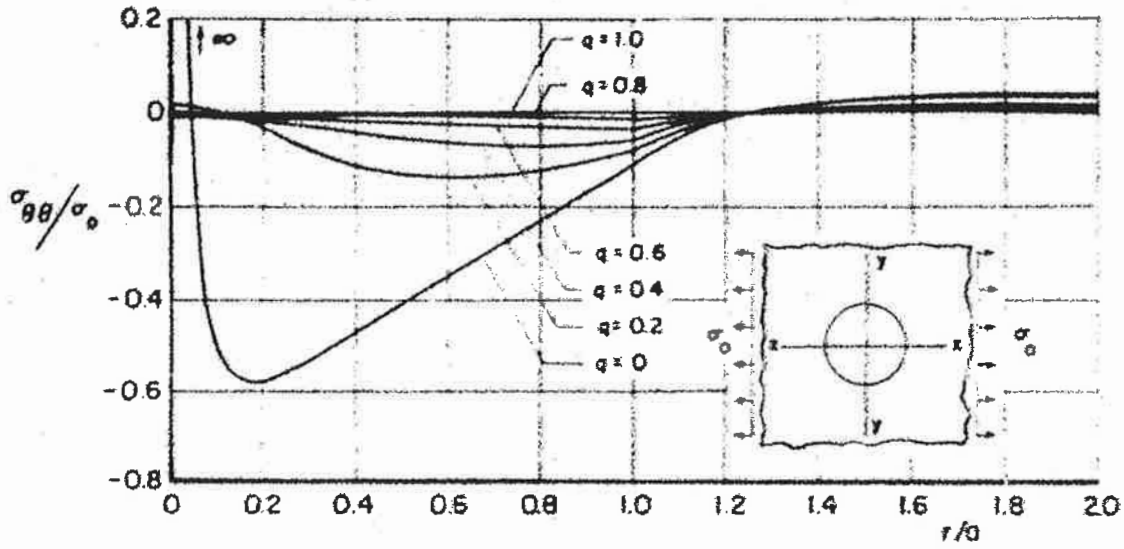

FIG. 6(a) TANGENTIAL STRESS ON X-X

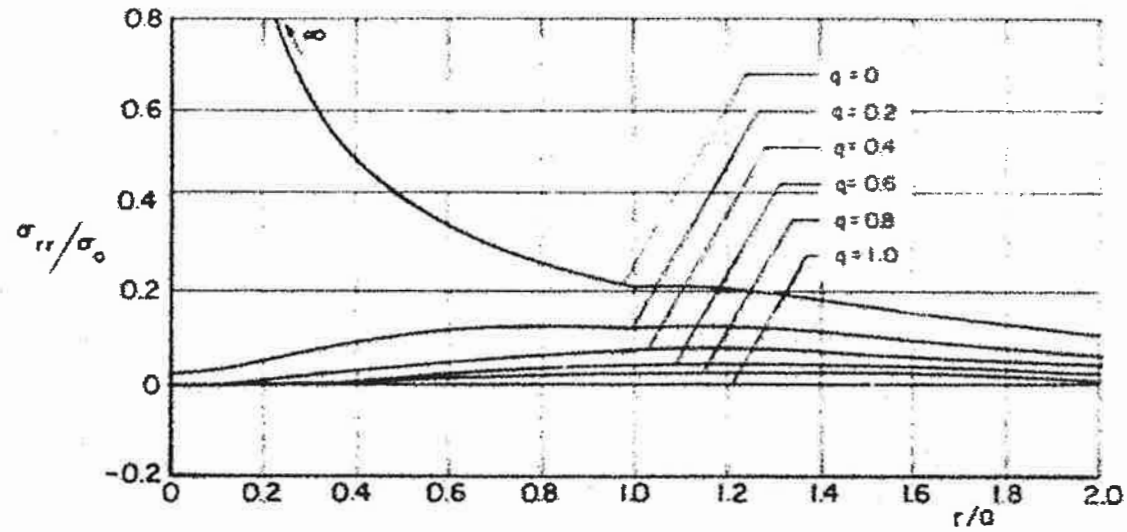

FIG. 6(b) RADIAL STRESS ON Y-Y

FIG. 7
LR-340

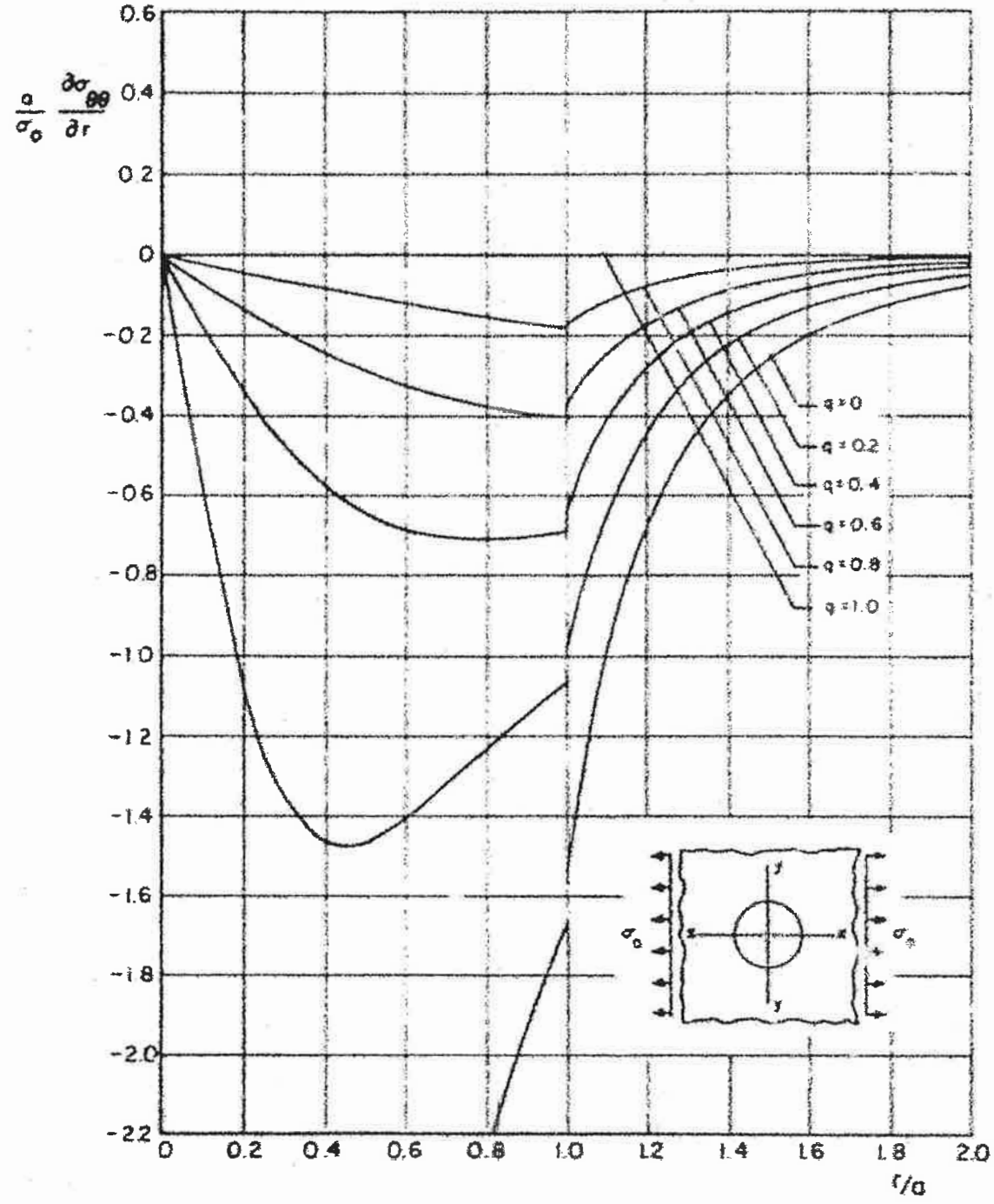

GRADIENT OF TANGENTIAL STRESS ON Y-Y

FIG. 8
LR-340

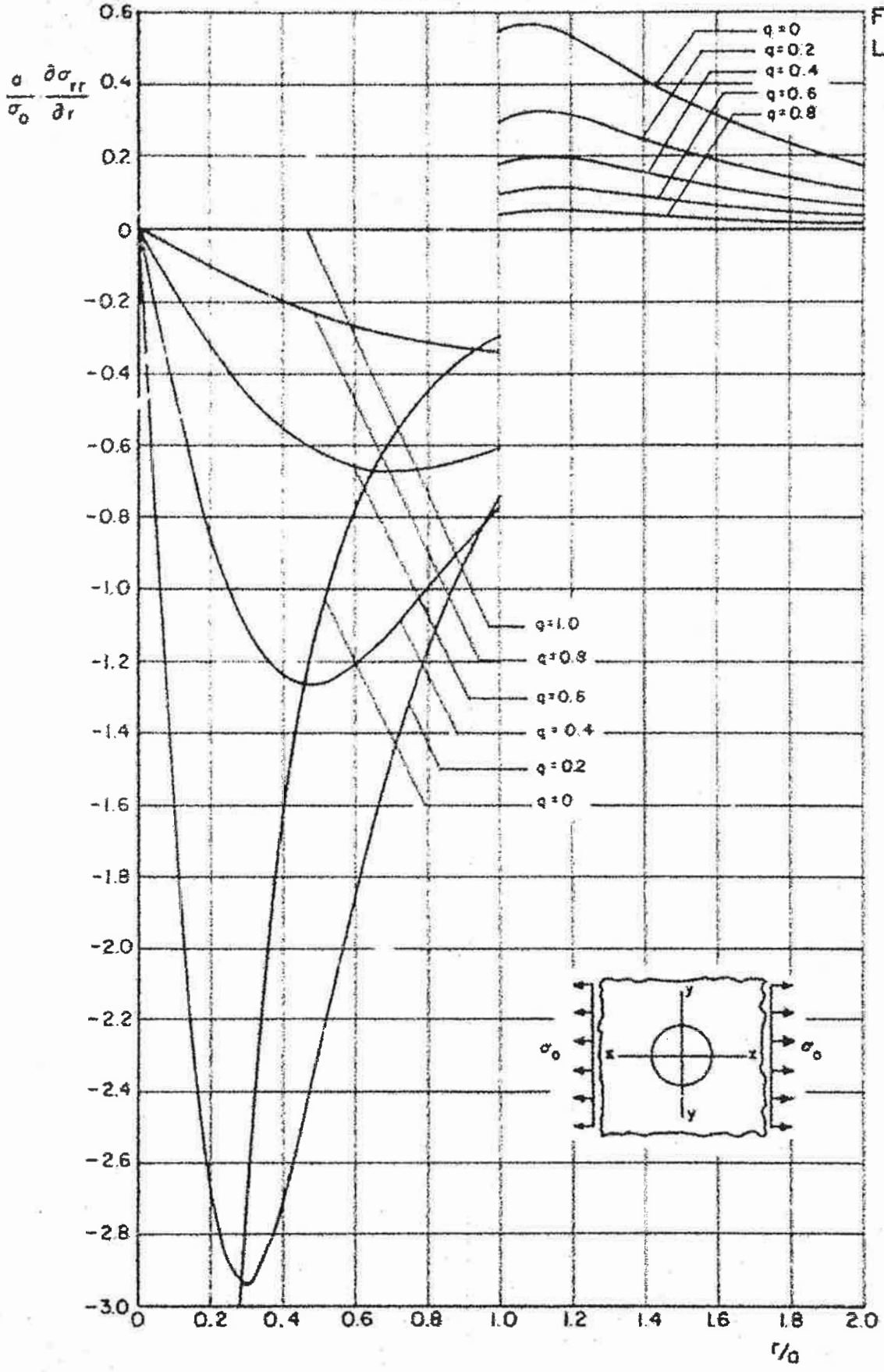

GRADIENT OF RADIAL STRESS ON X-X

FIG. 9
LR-340

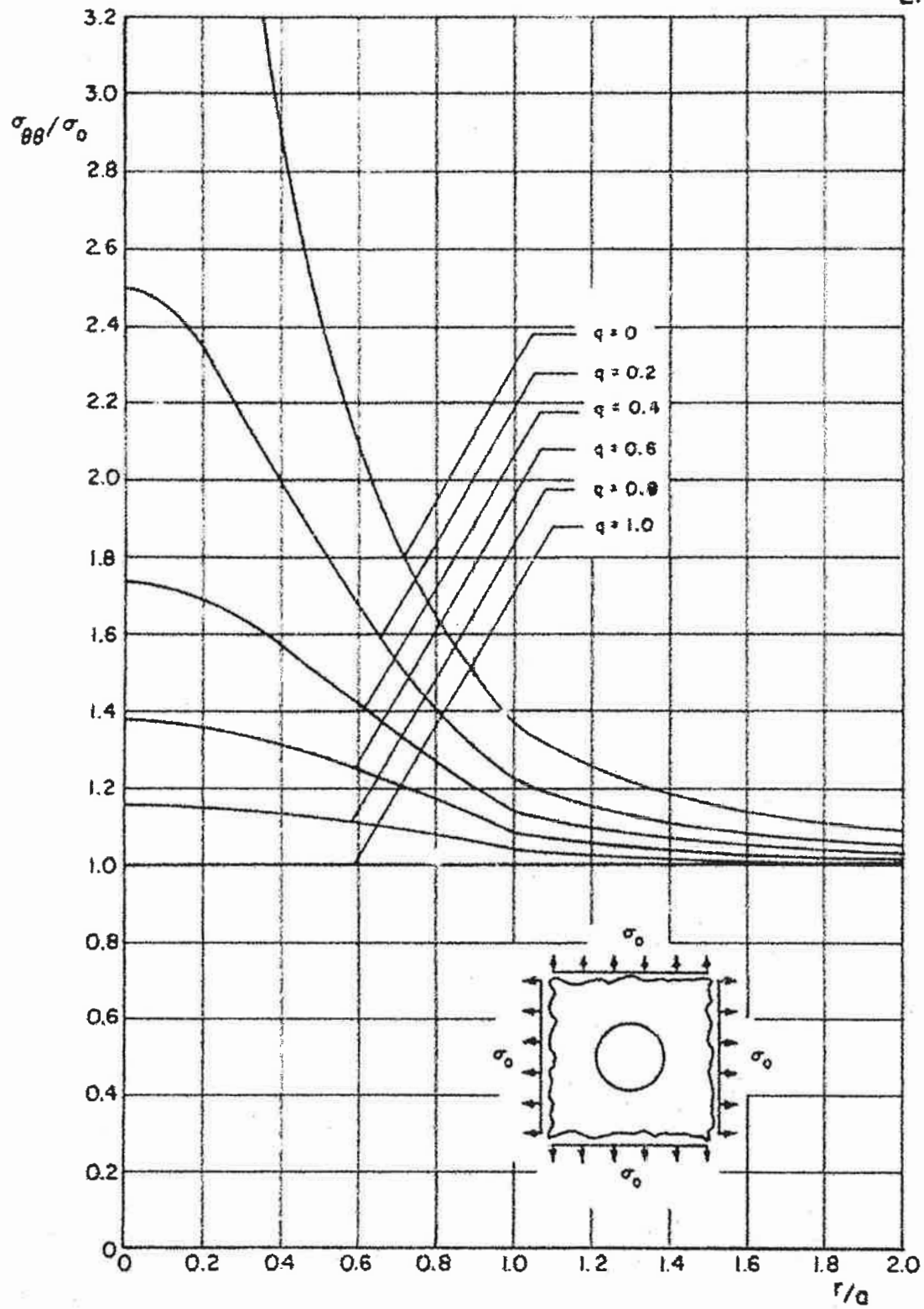

TANGENTIAL STRESS FOR UNIFORM BIAXIAL TENSION AT INFINITY

FIG. 10
LR-340

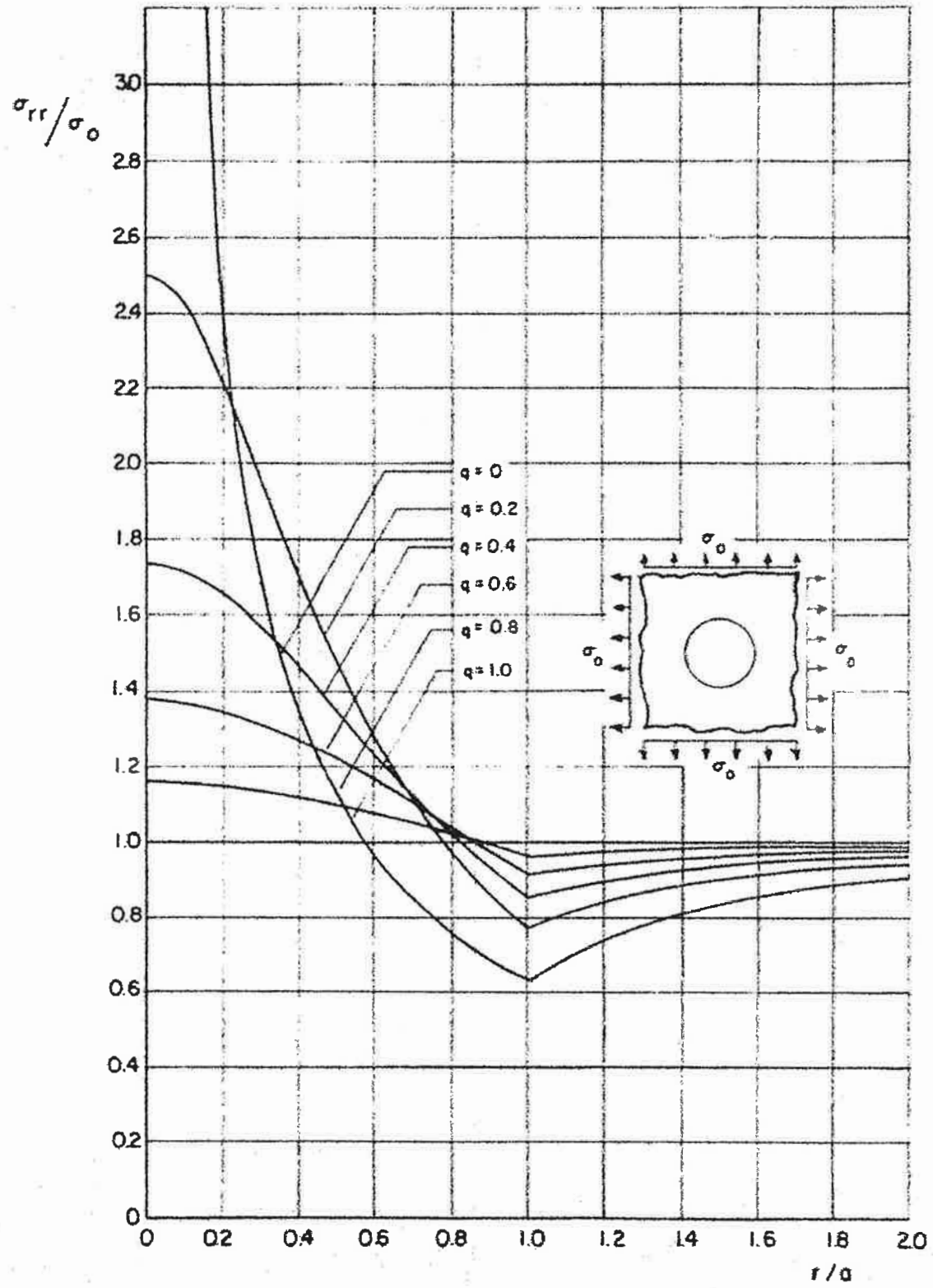

RADIAL STRESS FOR UNIFORM BIAXIAL TENSION AT INFINITY

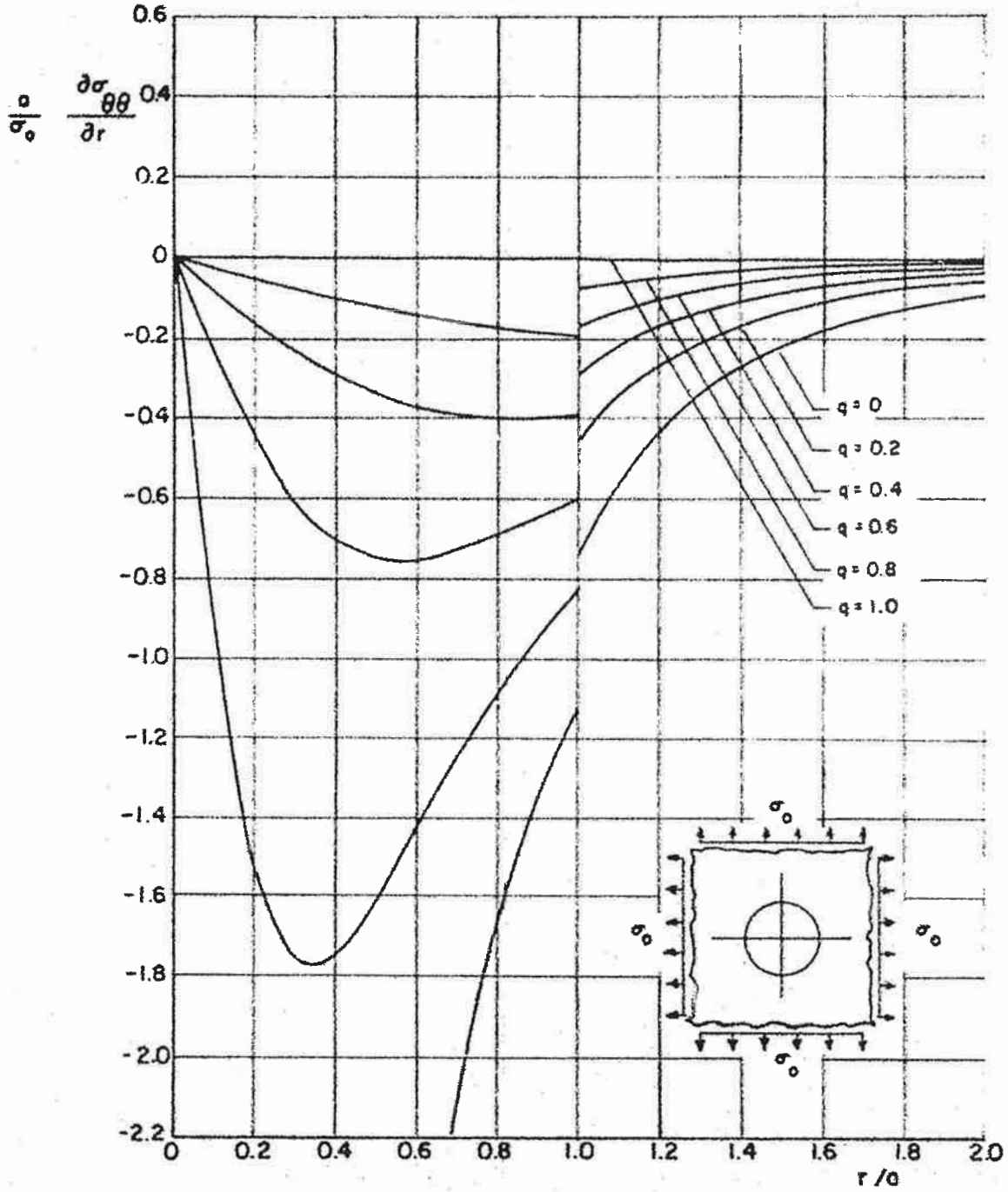

GRADIENT OF TANGENTIAL STRESS
FOR BIAXIAL TENSION AT INFINITY

FIG. 12
LR-340

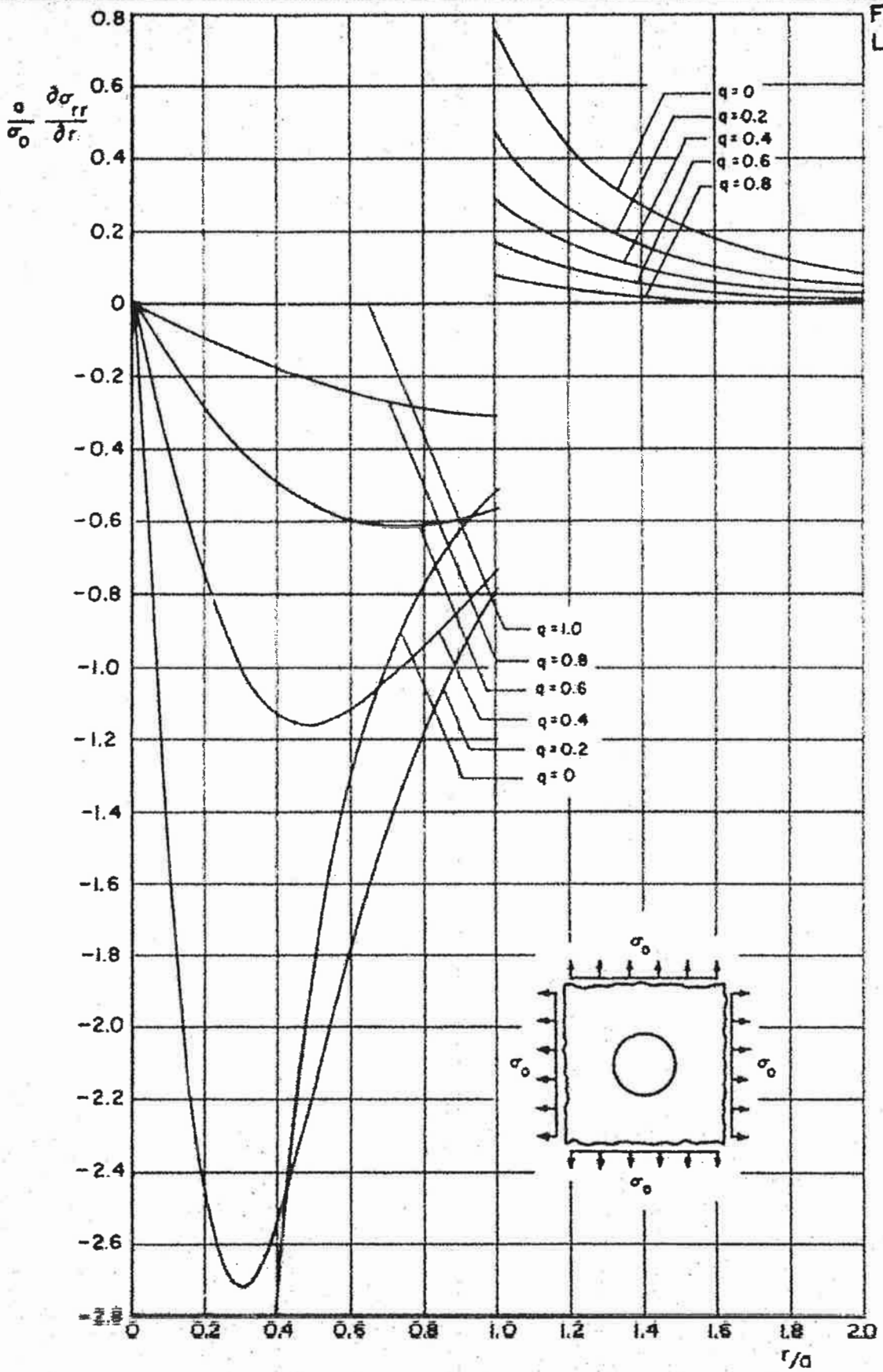

GRADIENT OF RADIAL STRESS FOR UNIFORM BIAXIAL TENSION AT INFINITY

FIG. 13
LR-340

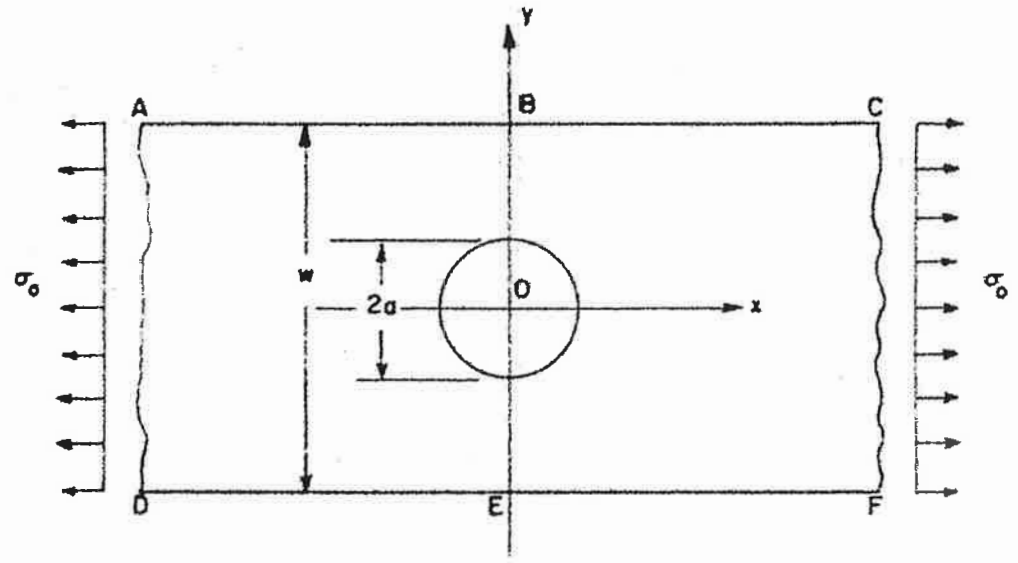

(a)

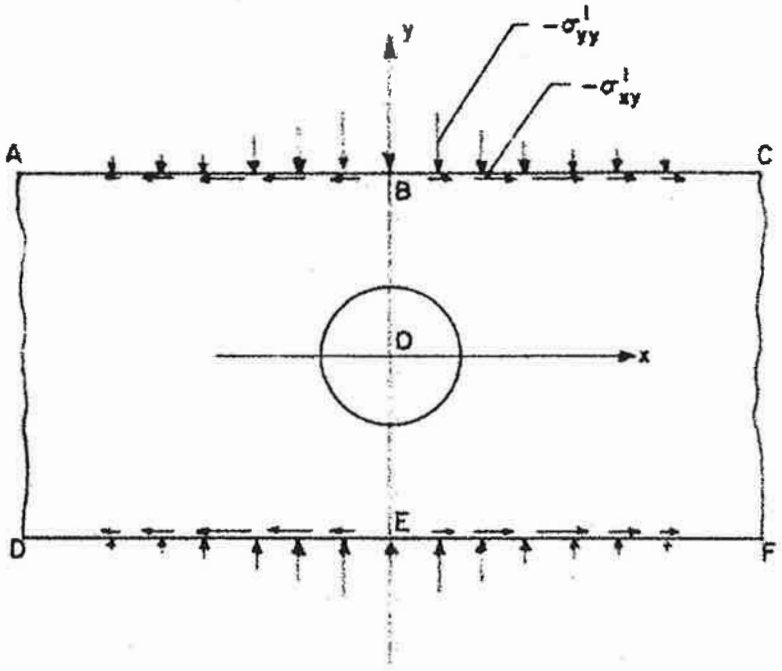

(b)

PLATE OF FINITE WIDTH

FIG. 14
LR-340

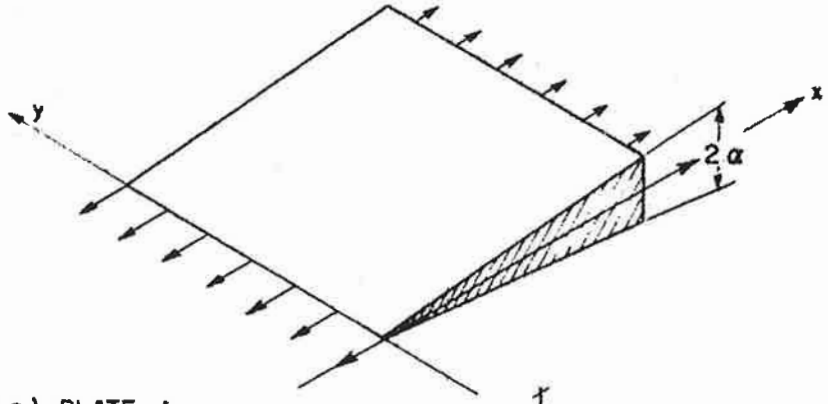

(a) PLATE A

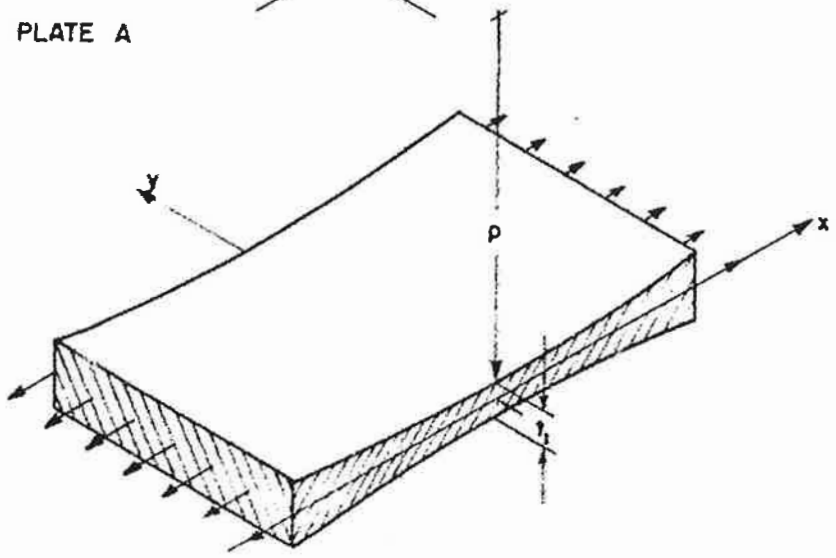

(b) PLATE B

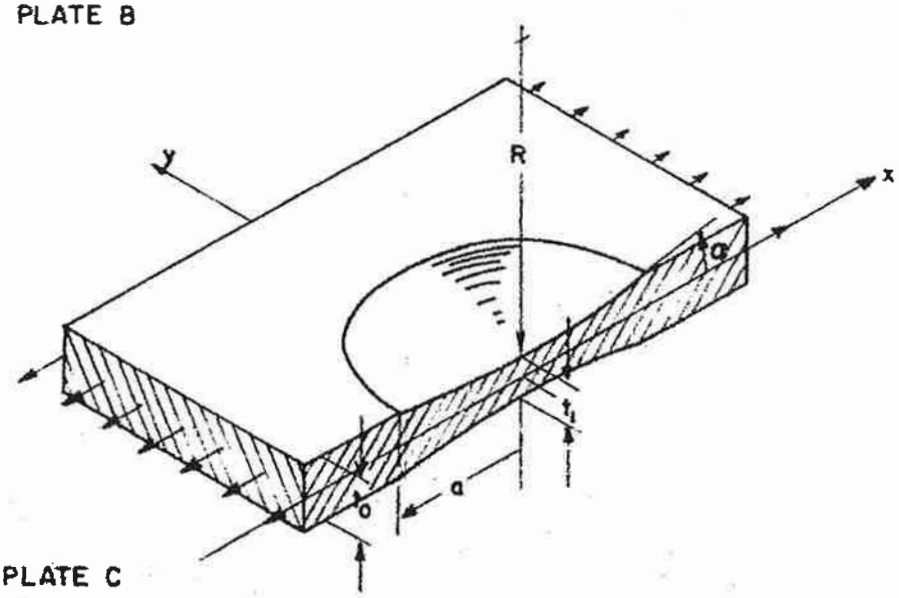

(c) PLATE C

PLATES FOR WHICH EXACT SOLUTIONS ARE AVAILABLE